MAX-PLANCK-INSTITUT FÜR PLASMAPHYSIK

GARCHING BEI MÜNCHEN

Improvement of the SUPERCOIL System Code

Part I

(stability of force-cooled superconductors, a.c. losses, and nuclear heat deposition)

M. Söll

IPP 4/225 November 1985

Die nachstehende Arbeit wurde im Rahmen des Vertrages zwischen dem Max-Planck-Institut für Plasmaphysik und der Europäischen Atomgemeinschaft über die Zusammenarbeit auf dem Gebiete der Plasmaphysik durchgeführt.

Abstract

This report describes the areas of the NET contract NET/84-042/PH which relate to problems of cooling and heat deposition in superconducting coils.

The areas have to be integrated as extensions into the SUPERCOIL computer program /18/; they are

- analytical model for force cooling of superconducting magnets by supercritical helium
- analytical model of the a.c. losses in the TF and PF coil systems
- analytical model for the nuclear heat deposition at the inner edge of the TF coil
- extension of the bath-cooling concept for additional heating sources (besides the ohmic heating losses)

I. Model for force-cooled superconductors

1. Theoretical background

The simplest method of cooling superconducting coils is to immerse them in a pool of liquid helium. The helium has to absorb the energy of external and internal disturbances and thus stabilize the magnet. To guarantee stable operation, the magnet has to fulfill certain stability criteria, the so-called "bath-cooling criteria" /1-5/. (A detailed description of the bath-cooling stability criteria is given in Ref. /5/.)

The main disadvantages of the bath-cooling concept are:

- weak mechanical structure as a consequence of the relatively high helium content and arrangement of the cooling spacers,
- low electric breakdown of the magnet; this is a severe problem for magnets where ionizing radiation is present.

To avoid the disadvantages of the bath-cooling concept investigations were started to use the force-cooling concept with hollow conductors, already a standard technique in the application of normal-conducting magnets, for superconducting magnets as well. The first experimental tests with a hollow conductor were successfully carried out at CERN with the OMEGA magnet /6/.

Unlike the bath-cooling concept, the force-cooling concept has no stability criteria in simple analytical form. This is due to the inherently dynamic situation of force-cooled conductors, to the nonlinearities and to the nonlocal behaviour. The complex cooling processes and the interaction between the turbulently flowing bulk helium, the helium surface layer, which dominates the heat transfer, and the heat sources in the conductor are schematically simplified in Fig. 1, which is a modified diagram from /7/.

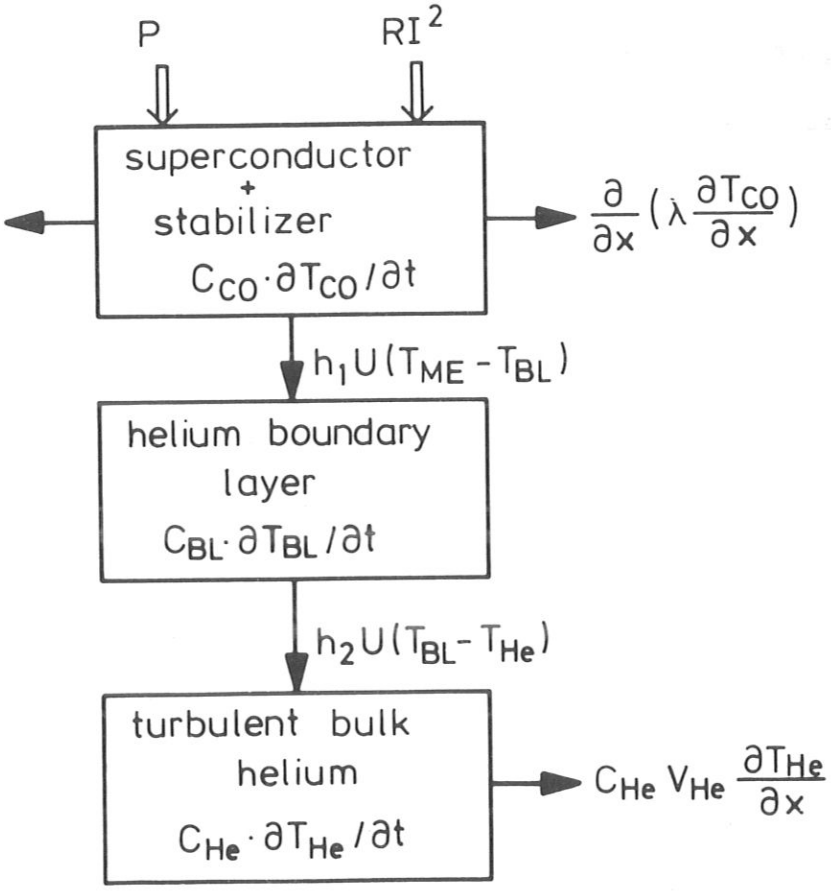

Fig. 1a Flow diagram of the heat from the sources (P_{ext}, RI^2) to the bulk helium.

The arrows show the heat flux direction.

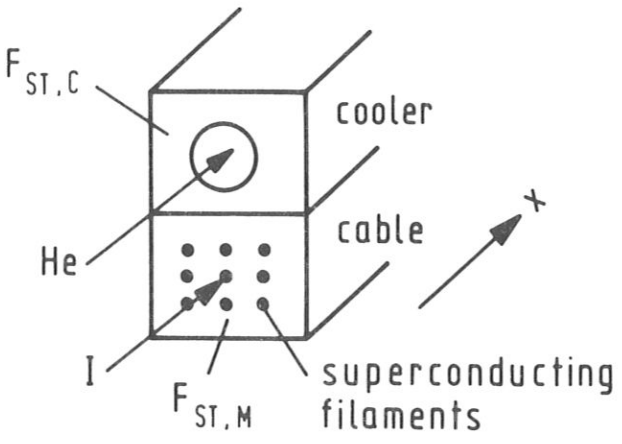

Fig. 1b: Schematic structure of a conductor with cable and cooler.

The heat sources are described by P_{ext} and RI^2, where P_{ext} stands for "external" sources, such as the nuclear heat deposited in the conductor, and RI^2 is the ohmic losses. The terms $C\,\partial T/\partial t$ describe the heat sinks due to heating of the material.

When transverse dependences are neglected (for a justification of this approximation see /7/), the behaviour of helium force-cooled conductor (including superconductor, stabilizer etc.) is described by the following set of differential equations:

$$C_{CO}\frac{\partial T_{CO}}{\partial t} - \frac{\partial}{\partial x}\left(\Lambda \frac{\partial T_{CO}}{\partial x}\right) + h_1 \cdot U \cdot (T_{CO} - T_{BL}) - I^2 R - P_{ext} = 0, \qquad (1)$$

$$C_{BL}\frac{\partial T_{BL}}{\partial t} - h_1 \cdot U \cdot (T_{CO} - T_{BL}) + h_2 \cdot U (T_{BL} - T_{He}) = 0, \qquad (2)$$

$$C_{He}\frac{\partial T_{He}}{\partial t} + C_{He} \cdot V_{He} \cdot \frac{\partial T_{He}}{\partial x} - h_2 \cdot U (T_{BL} - T_{He}) = 0, \qquad (3)$$

$$L\frac{\partial f}{\partial t} - R_T \frac{\partial^2 f}{\partial x^2} + (R_M + R_C) \cdot f - R_C = 0, \qquad (4)$$

$$\frac{\partial \gamma_{He}}{\partial t} + \frac{\partial}{\partial x}(\gamma_{He} \cdot V_{He}) = 0, \qquad (5)$$

$$\gamma_{He}\frac{\partial V_{He}}{\partial t} + \gamma_{He} \cdot V_{He} \cdot \frac{\partial V_{He}}{\partial x} + \frac{\partial P_{He}}{\partial x} = 0. \qquad (6)$$

The symbol x denotes the coordinate along the conductor axis (see Fig. 1b). All values in eqs. (2)-(4) are taken per unit length, with the exception of R_T. The indices CO, BL and He denote the conductor, the helium boundary layer and the turbulent bulk helium, respectively. The heat transfer from

the conductor surface to the helium boundary is given by the heat transfer coefficient h_1, and that from the helium boundry layer to the bulk helium by h_2. U is the cooled perimeter of the conductor and the heat capacitances C_{CO}, C_{BL} and C_{He} are abbreviations for

$$C_{CO} = c_{ST}\gamma_{ST}F_{ST} + c_R\gamma_R F_R + c_{SC}\gamma_{SC}F_{SC} + c_{SO}\gamma_{SO}F_{SO} + c_B\gamma_B F_B \,, \tag{7}$$

$$C_{BL} = c_{He}\gamma_{He}d_{BL}U \,, \tag{8}$$

$$C_{He} = c_{He}\gamma_{He}F_{He} - C_{BL} \,. \tag{9}$$

F is the cross-sectional area, c is the specific heat per volume and γ is the specific mass. The indices used in the relation (1)-(9) are abbreviations for:

ST = stabilizer, SC = superconductor, R = reinforcing material (steel), SO = solder, B = high-resistance boundaries (CuNi), He = helium, CO = conductor, BL = boundary layer; d_{BL} is the helium layer thickness.

The thermal conductance Λ per unit length in the conductor (see eq. (1)) is related to the thermal conductivity λ by

$$\Lambda = \lambda_{CO}F_{CO} \tag{10}$$

and the electrical resistances R_M and R_C (per unit length) in the normal-conducting state by

$$R_M = \rho_{ST}/F_{ST,M} \,, \quad R_C = \rho_{ST}/F_{ST,C} \tag{11}$$

The definitions of R_M and R_C are based on the following model. The cross-sectional area for high-current superconductors is usually made from smaller sub-units, as shown schematically in Fig. 1b. The sub-units are the superconducting cable and the cooling structure. The superconducting cable consists of the superconducting filaments and a small amount of stabilizing material; the cooling structure consists of stabilizing material. The electrical resistance can thus be subdivided into two parts, into the resistance of the cable denoted as R_M and the resistance of the cooling structure R_C. With respect to this subdivision, a current distribution factor f can be defined, $f = I_M/I$ (I_M is the current flowing in the cable and I is the total current). In eq. (4) there are two further values, namely R_T and L. R_T is the specific transverse resistance ($\Omega \cdot m$) and L is the inductance per unit length of the total conductor.
In the following, a short description of eqs. (1)-(6) is given and the procedure is described how to get an "analytical" approximation of the system of equs. (1)-(6).

Equation (1) is the heat balance equation of the conductor. The terms in eq. (1) are the enthalpy change in the conductor, the heat transfer to the helium boundary layer, the ohmic heating of the conductor and the external disturbance (the expression "external" is in a sense misleading nomenclature because other mechanisms such as a.c. fields /5/ and nuclear radiation and dynamic stresses /8/ provide heat in the conductor).

Equation (2) is the heat balance equation of the helium surface layer; the terms are the enthalpy change in the (laminar) helium boundary layer, the heat transfer from the conductor and the heat transfer to the turbulent helium.

Equation (3) describes the heat balance of the turbulent bulk helium; the terms are the enthalpy change in the turbulent bulk helium, the convective longitudinal heat transport and the heat transfer from the laminar boundary layer.

Equation (4) describes the dynamics of the current transfer inside the conductor after a temperature excursion above critical values. Current then flows from the superconducting filaments into the stabilizing material; the current does not immediately spread over the whole copper cross-setion, but remains in the cable (see Fig. 1b) at first. In other words, the current is at first concentrated near the filaments before the transfer takes place across the total stabilizer cross-section $F_{ST.M} + F_{ST.C}$. The current transfer takes place with a time constant given by the inductances and resistances of the cable and cooling structure. The steady state is obtained after the current is distributed homogeneously across the total stabilizer material. The current distribution is described by the factor f (current distribution factor), $f = I_n/(I_c+I_M)$ /7,9/. (I_M current in the cable, I_c current in the cooling structure.)

Current flows from the superconducting filaments into the stabilizer when the saturation temperature T_s is exceeded. The saturation temperature is defined as the highest temperature at which a superconducting cable etc. can carry at a given external magnetic field the transport current I without losses (T_s is often designated in the literature also as the current-shearing temperature). As can be seen from eqs. (26) and (29), T_s is in the range between the cooling temprature T_{He} and T_c, depending on the transport current; $T_s = T_{He}$ if $I = I_c$, where I_c is the critical current

(I_c is the maximum current which can flow in a superconductor at a given B and T without losses and is given by $j_c(B,T) \cdot F_{SC}$). If the transport current is I = 0, the saturation temperature coincides with the critical temperature T_c.
The behaviour of the helium inside the conductor is described by the continuity equation (5) and by the force equation (6).

The solution of the system of equations (1-6) can only be carried out by numerical methods; several authors have developed computer programs for this purpose /6, 7, 9, 11-14/; the models differ with respect to some approximation but all include the transient effects. In some cases the computer programs were tested with experimental results /10/, especially for the development of the LCT conductor /15, 16/.

A detailed comparison of measurements and numerical calculations were carried out by Junghans /7, 9, 10/.

Within the framework of the SUPERCOIL computer program it would be too time-consuming to solve the system (1)-(6) of space and time-dependent equations. Instead we use the time-integrated global energy equation of the conductor, helium layer and bulk helium, which is obtained by adding eqs. (1) to (3) and integrating with respect to space and time. Volume integration is over the disturbance zone x, and it is assumed that the x-dependence can be neglected. (One exception has to be noted. In calculating the energy Q_L (see eqs. 19 and 20) a linear temperature profile along the disturbance zone is assumed):

$$\int C_{CO}\,dT_{CO} + \int C_{BL}\,dT_{BL} + \int C_{He}\,dT_{He} + \int C_{He} V_{He} \frac{dT_{He}}{dx}\,dt = \int \left[I^2 R + P_{ext} \right] dt \qquad (12)$$

In evaluating the terms in eq. (12) a flat temperature profile in the conductor and a temperature gradient in the helium boundary layer is assumed. The temperature of the bulk helium is assumed to increase from the beginning of the disturbance zone from $T = T_{He,i}$ to $T = T_{He,i} + \Delta T_2$ at the end of the disturbance zone; a linear dependence is assumed. Equation (4) is taken into account in the model by using steady state values for the current distribution depending on the temperature. For $T < T_S$ the current flows in the superconductor for $T_s < T < T_c$, the ohmic heating power P_Ω increases linear (see Appendix II) and for $T > T_c$ the P_Ω is given by I^2R, where I is the conductor current and R the resistance (per unit length). Through the assumption of quasistationarity in x-direction eqs. (5) and (6) disappear.

The conductor (including the cooling medium) can take up a certain amount of energy without loosing the superconducting state. The limiting value is denoted as the critical energy Q_c. If an energy larger than Q_c is produced or deposited in the conductor, uncontrollable propagation of the normal-conducting state takes place; such uncontrolled propagation is denoted as a quench. The left-hand side of eq. (12) describes the "energy sinks", and the right-hand side the "energy sources". The maximum of the sum given by the terms of the left-hand side defines the critical energy Q_c.

In the following, the explicit expressions for the left-hand side terms are given and discussed.

The first term (Δx is the length of the disturbance zone)

$$Q_{CO} = \Delta x \int_{T_{He,i}}^{T_s} C_{CO}\, d\bar{T}_{CO} \tag{13}$$

is the energy which is taken up by the conductor itself. The temperature integral is taken from the helium inlet temperature $H_{He,i}$ up to the saturation temperature T_s. Under a given operating condition when the Stekley parameter α_s (see below) is greater than one, the saturation temperature cannot be exceeded without a quench; in these cases, the heat produced in the conductor when $T > T_s$ is (roughly speaking) always larger than the heat which can be cooled away by heat transfer across the helium layer. It should be noted that Q_{CO} does not depend on the duration of the disturbance.

The second term in eq. (11) describes the energy carried away by the transient heat transfer:

$$Q_{BL} = \Delta x \int C_{BL}\, d\bar{T}_{BL} \,. \tag{14}$$

For heat pulses $\Delta t > 10$ ms, Q_{BL} approaches a limiting value /7, 9/

$$Q_{BL}^{\infty} = C_{BL}\, \Delta x\, \frac{T_s - T_{He,i}}{2} \tag{15}$$

which is determined by the heat capacity C_{BL} of the boundary layer (see eq. (8)).

The factor 1/2 follows from the fact that in the steady state the average temperature of the helium boundary layer is half the temperature difference

between the conductor and the (turbulent) bulk helium. The helium layer thickness d_{BL} is correlated with the steady-state heat transfer h_s by

$$d_{BL} = \lambda_{He} / h_s , \tag{16}$$

where λ_{He} is the thermal conductivity of the helium. For fast disturbances ($\Delta t < 1$ ms) the heat transfer coefficient h varies with time /9, 17/; analytically, an $h \sim t^{-1/2}$ dependence was found /17/.

The third term in relation (11) describes the heat transferred away by the bulk helium:

$$Q_S + Q_L = \Delta x \left[\int C_{He}\, dT_{He} + \int C_{He} v_{He}\, dT_{He}/dx\, dt \right] \tag{17}$$

For long disturbance duration the steady-state heat transfer is dominant. The energy transferred away by the steady-state bulk helium is given by /7, 9/

$$Q_S = \frac{\overline{T}_S - \overline{T}_{He,i}}{\frac{1}{h\, U\, \Delta x} + \frac{1}{\dot{m}\, c_{He}}} \cdot \Delta t \tag{18}$$

($\dot{m}$ is the helium mass flow and c_{He} is the specific heat of helium). Before the steady-state heat transfer is reached, a steady-state temperature profile has to be built up (see Fig. 21 in Ref. /10/). The energy needed is given by /10/

$$Q_L(\Delta t) = Q_L^{\infty}\,[1 - \exp(-h\,U\,\Delta t / C_{He})], \tag{19}$$

with

$$Q_L^{\infty} = \frac{C_{He}\,\Delta x}{2} \cdot \frac{h\,U\,\Delta x\,(T_S - T_{He,i})}{\dot{m}\,c_{He} + h\,U\,\Delta x}\,. \tag{20}$$

The critical energy Q_c is the sum of the four terms (13), (14), (19), (20):

$$Q_c = \sum_4 Q_i = Q_{CO} + Q_{BL} + Q_S + Q_L\,. \tag{21}$$

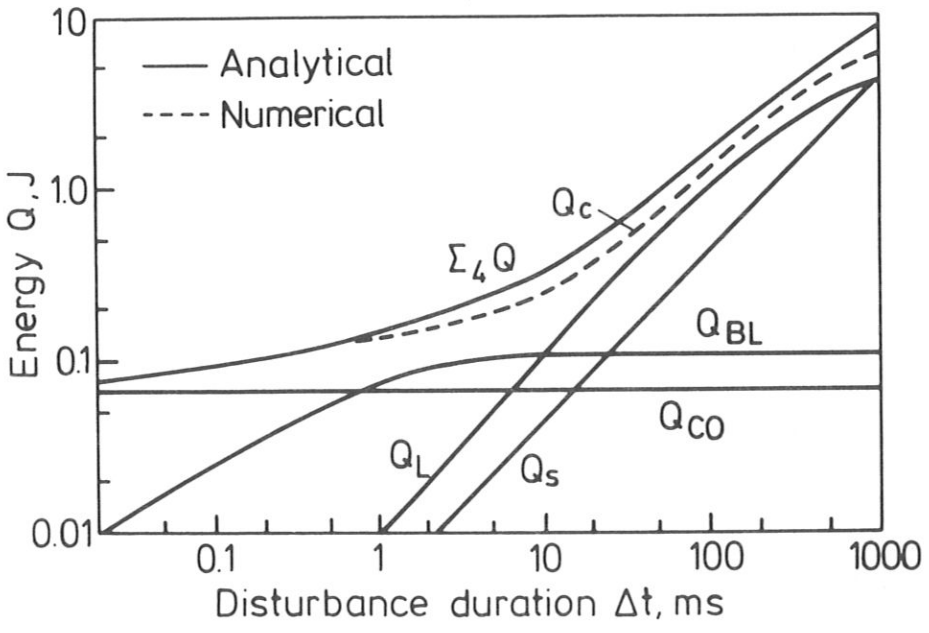

Fig. 2: Comparison of numerically (curve Q_c) and analytically (curve $\sum Q$) calculated critical energies /10/.

The question of the accuracy of the analytical model, in which the

effects of the transient helium flow are neglected (which follow primarily from the continuity and force equations), was investigated by Junghans /10/. An example of a "bundle" conductor is given in Fig. 2. The critical energy calculated analytically and numerically differ only moderately. He also compares numerically calculated Q_c values with experimental ones /7, 9, 10/. He found that the measured values of the critical energy are in good agreement with the calculated ones; the analytical model is thus a suitable model to describe force-cooled superconductors for a rough conductor design.

The expression for the critical energy Q_c attained is valid for cases where the Stekly parameter α_s /1, 5/ (generally the Stekly parameter is denoted by α ; we change the notation to α_s because in our SUPERCOIL program /18/ we used the symbol α for the cross-section ratio between the stabilizer and superconductor) is larger than 1. The Stekly parameter is defined for bath-cooled conductors with only ohmic heating losses as

$$\alpha_s = \frac{I^2 R}{h\, U\, (T_c - T_{He,i})} \quad . \tag{22}$$

With additional heating losses P_1, P_2 .. (a.c. losses etc.) α_s is given by

$$\alpha_s = \frac{I^2 R + P_1 + \ldots + P_n}{h\, U\, (T_c - T_{He,i})} \quad . \tag{22'}$$

The parameter α_s is the ratio between the heat produced in the normal-conducting conductor (per unit length) and the heat transferred to the liquid helium. If the heat I^2R produced can be transferred into the helium at the temperature difference $T_C - T_{He}$ the conductor is in a stable operation

condition. The conductor is then restored in the superconducting state after an excursion to the normal conduction state. From this it follows that recovery and therefore stable operation is obtained for $\alpha < 1$. The parameter α_s separates the stable from the unstable operation regimes. This definition describes unequivocally the stability behvaiour of a bath cooled superconductor.

For force-cooled conductors the situation is more complex, because in contradiction to the condition of bath cooling the helium temperature, heat transfer coefficient etc. changes /7, 10/. (A simple elementary theory of the stability of force-cooled superconductors with respect to α_s can be found in Ref. /20/.)
Nevertheless α_s gives for force-cooled conductors a rough characterization of the conductor. For $\alpha_s > 1$ no ohmic heating is allowed ($T_{CO} < T_s$) because between T_s and (including) T_c the heat produced by the current is larger than the additional heat transferred to the helium. As can be shown the additional heat RI^2 produced by a temperature increase from T_s to T ($T = T_s + \Delta T$) is larger than the additional heat transferred to the helium (see Appendix II), if an optimized conductor is used where the external heat $P_1 + \ldots + P_n$ is equal to the critical energy. .

For conductors with $\alpha_s \leq 1$ the critical energy is enhanced by Q_K /7/:

$$Q_K = \int C_{He} (1 - \alpha_s)^2 (T_c - T_{He,i}) - I^2 R \Delta t \, \Big] \Delta x \qquad (23)$$

As can be seen from eq. (23), the additional heat sink (turbulent helium) is only effective for short durations; for durations in the range of

seconds as for fusion reactors with heat loads in the second range (a.c. losses, nuclear heat), there is almost no improvement with respect to conductors with $\alpha_s > 1$.

In conclusion, the stability of force-cooled conductor can be expressed by the condition that the critical energy Q_c has to be larger than the energy inducing the disturbance:

$$Q_c = Q_4 = \sum_4 Q_i \quad , \qquad \alpha_s > 1 \quad , \tag{24}$$

$$Q_c = Q_5 = \sum_4 Q_i + Q_K) \qquad \alpha_s \leq 1 \quad .$$

2. Description of the model

In the last section the formulae defining the critical energy and disturbances are given in general form. In this section the formulae are specified with respect to the material properties, conductor concept and conductor geometry.

The model for force-cooled superconductors (notation FORCED) should be integrated into the SUPERCOIL program /18/, a system code for tokamaks with superconducting TF coils. It is evident that for such a purpose the solution of the total system of equations (1-6) is too time-consuming and complex; we prefer the analytical model as a subsystem of SUPERCOIL.

The FORCED program is conceived for three conductor types (see Fig. 3): a so-called cable-in-conduit conductor (or cable) and two hollow conductors with different cooling channel geometries (further denoted as conductors I, II, III).

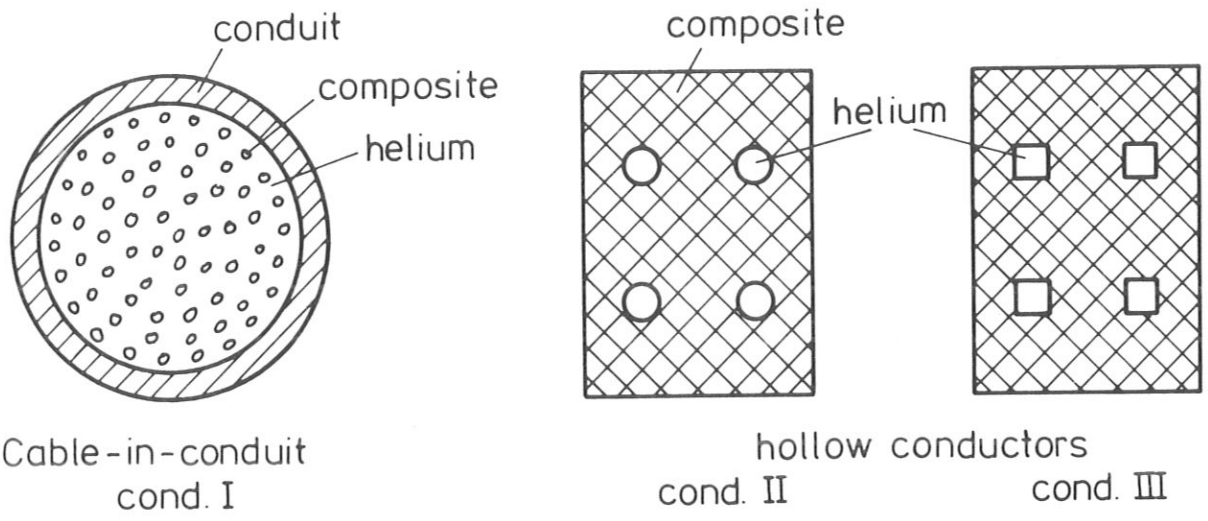

Fig. 3: Schematic view of conductors used in FORCED

In general, conductor I consists from a stainless steel conduit and superconducting strands located within the conduit. The strands are either superconducting filaments (without copper) or they are composites with a small fraction of copper. The stability of such conductors can be improved by using helium under large pressure (large heat capacity) or by using additional copper wires which are galvanically coupled to the superconducting strands.

The general structure of the conductors II and III is shown by Fig. 1b. There is a cable with the superconducting filaments and a part with stabilizing material and the cooling channels (cooler).

The FORCED program is designed for the two commercial superconductors NbTi and Nb_3Sn.

The critical temperature T_c, the saturation temperature T_s and the critical current density are described in /21, 22/. (In the formulae (26)-(30) T_{He} is identical to $T_{He,i}$, the nomenclature used before.)

For NbTi:

$$T_c = 9.2\ (1-B/14.7)^{1/2}, \tag{25}$$

$$T_s = (T_c-T_{He})(1-I/I_c) + T_{He}, \tag{26}$$

$$j_c = (T_c-T_{He})(3.352-0.3607\ B + 11.929/T_{He}) \times 10^8 \tag{27}$$

For Nb_3Sn:

$$T_c = 18.30 \times (1-B/24.0)^{1/2}, \tag{28}$$

$$T_s = (T_c-T_{He})(1-I/I_c) + T_{He}, \tag{29}$$

$$j_c = (35.55-4.25\times B + 0.1375\times B^2)(0.739+0.144\times T_{He} - 0.0196 \times T_{He}^2) \times 4.74 \times 10^8. \tag{30}$$

The specific heats (for the calculation of Q_{CO}) for the superconductors, stabilizers and the solder are given in FORCED as polynomials derived by a fit program from the figures in /5, 11/.

For the superconductors NbTi and Nb_3Nb:

$$c_p = 1.8899\times10^{-3} + 2.5612\times10^{-1}\ T - 3.8366\times10^{-2}\ T^2 + 8.4492\times10^{-3}\ T^3 - 2.5767\times10^{-4}\ T^4, \tag{31}$$

$$c_p = 2.4479\times10^{-3} - 9.9249\times10^{-2}\ T + 3.6128\times10^{-2}\ T^2 - 1.409\ \times10^{-3}\ T^3 + 1.8472\times10^{-4}\ T^4. \tag{32}$$

For the stabilizer materials Cu and Al:

$$c_p = -2.3774\times10^{-6} + 2.7122\times10^{-3}\ T + 4.0381\times10^{-3}\ T^2 + 1.4296\times10^{-4}\ T^3 + 2.1168\times10^{-5}\ T^4. \tag{33}$$

$$c_p = -5.9987\times10^{-4} + 1.0817\times10^{-1}\ T - 2.4012\times10^{-2}\ T^2 + 3.4099\times10^{-3}\ T^3 - 7.4002\times10^{-5}\ T^4, \quad (34)$$

For the solder:

$$c_p = 6.6038\times10^{-3} - 1.0008\times10^{-1}\ T - 3.3053\times10^{-2}\ T^2 + 2.9956\times10^{-2}\ T^3 - 1.1710\times10^{-3}\ T^4. \quad (35)$$

The specific heat per volume follows from the c_p-values of eqs. (31-35) by multiplication by the mass density; the values used are in the sequence of the c_p-functions:

5.6×10^3, 8.9×10^3, 8.962×10^3, 2.698×10^3, 10^4.

The specific resistivities of copper and aluminium are given by /24,25/

$$\rho_e^{Cu} = (2 + 0.36\,B)\cdot 10^{-10} + 4.4\cdot 10^{-9}\left[1 - \exp(-1.6\cdot 10^{-23}\varphi)\right], \quad (36)$$

$$\rho_e^{Al} = 10^{-10} + 9.4\cdot 10^{-9}\left[1 - \exp(-2.8\cdot 10^{-23}\varphi)\right], \quad (37)$$

where φ is the neutron dose. For the conductors behind the shielding (with thickness D) the neutron flux is calculated from

$$\varphi_{in} = 4.427 \times 10^{17}\ N_n\ e^{-14.00\ D} \quad (38)$$

(N_n is the mean neutron wall load in MW/m²)

$$F_m^{Cu} = 8.962\cdot 10^3 \int_{T_{He,i}}^{T_m} \frac{c_p^{Cu}(T)\,dT}{\rho_e^{Cu}}, \quad (39)$$

$$F_m^{Al} = 2.698\cdot 10^3 \int_{T_{He,i}}^{T_m} \frac{c_p^{Al}(T)\,dT}{\rho_e^{Al}}. \quad (40)$$

F_m^{Cu} and F_m^{Al} follow from safety discharge analysis /2/. The maximum allowable temperature of the conductor after a safety discharge is T_m. With formulae (36) and (37) for ϱ_e, T_m should not exceed about 50 K because there the resistivity is taken as temperature-independent.

$$\alpha F_m^{SC} + \alpha^2 F_m^{ST} + \alpha \cdot \gamma \cdot F_m^{SO} = j_c^2 \cdot IK^2 / (V_m \cdot I) \qquad (41)$$

IK is the ratio between the nominal conductor current I and the critical current $I_c(B,T_{He})$, V_m is the maximum discharge voltage and E_m is the stored magnetic energy. With the parameter α the ratio F_{ST}/F_{SC} (F_{ST} cross-sectional area of the stabilizer, F_{SC} cross-sectinal area of the superconducting material) is determined; the ratio α calculated with eq. (41) is a minimum value following from the safety discharge analysis (see Appendix I).

$$F_{sc} = I_c / j_c = I / (j_c \cdot IK) \qquad (42)$$

The energy Q_{CO} is calculated by

$$Q_{CO} = \Delta x \, F_{sc} \int_{T_{He,i}}^{T_s} [C_{sc} + \alpha C_{ST} + \gamma C_{SO}] \, dT \qquad (43)$$

$\gamma = F_{SO}/F_{SC}$ is the normalized cross-sectional area of the solder, Δx the perturbation length . In rel. (43) the reinforcing material (stainless steel or aluminium alloy) and CuNi barriers are not taken into account. For the conductors considered (Fig. 3) the reinforcing material is separated from the conductor by electrical insulation layers, which act as thermal barriers. The low and high-resistance electrical barriers of CuNi (to reduce a.c. losses) are neglected.

The material functions for the supercritical helium which are used in the FORCED program are the specific density ρ_{He}, the specific heat c_{He}, the thermal conductivity λ and the viscosity η; all four material functions depend on the pressure and temperature /17, 26/. The material values are calculated with the data listed in Tables 1-4; for the temperature and pressure in the disturbance zone mean values $\bar{T}$ and $\bar{P}$ are used:

$$\bar{T} = (T_{He,i} + T_s)/2 \quad , \tag{44}$$

$$\bar{P} = P_{He,i} - \Delta P/2 \quad . \tag{45}$$

The interpolation between the fixed points (given in the Tables 1-4) are carried out with cubic spline functions.

$P_{He,i}$ is the pressure at the conductor inlet and ΔP is the pressure drop across the disturbance zone (which in our simplified model is constant in length).

In the following the indices I, II and III characterizing the three different conductor configurations are shown in Fig. 3 (I: cable-in-conduit; II: hollow conductor with circular cooling channels; III: hollow conductor with squared cooling channels)

$$D_I = 2\delta \frac{\sqrt{F_{sc}}}{[\pi(1+\alpha)n]^{1/2} + [\pi(1+\alpha+\gamma+\delta)]^{1/2}} \quad , \tag{46}$$

$$D_{II} = 2\left[\frac{\delta \cdot F_{sc}}{n\pi}\right]^{1/2} \quad , \tag{47}$$

$$D_{III} = \left[\frac{\delta \cdot F_{sc}}{n}\right]^{1/2} \quad . \tag{48}$$

D is the hydraulic diameter of the conductor with n strands (for conductor I) or n cooling channels (for conductors II, III)

$$U_{\underline{I}} = 2\left[F_{sc} (1+\alpha) n \pi \right]^{1/2} , \tag{49}$$

$$U_{\underline{II}} = 2\left[n \pi \delta \cdot F_{sc} \right]^{1/2} , \tag{50}$$

$$U_{\underline{III}} = 4\left[n \delta F_{sc} \right]^{1/2} \tag{51}$$

(cooled perimeter of the conductor).

$$Re_{I,II,III} = \left[\frac{2 \gamma_{He} \cdot \Delta P \cdot 10^5 \, D^3_{I,II,III}}{f_1 L \eta^2} \right]^{1/(2+f_2)} \tag{52}$$

(ΔP in bar).

R_e is the Reynold's number. The parameters f_1 and f_2 determine the friction factor f

$$f = f_1 Re^{f_2} \tag{53}$$

which for complex systems is like a bundle conductor found from experiments. For smooth tubes, values for f_1 and f_2 can be found in the literature (e.g. /28/).

(The friction factors f depend on the structure of the conductor; for complex conductors, generally the friction factor f is found from experiments; see, for instance, /16/; if layout calculations with FORCED

are carried out, one should take care that the factors f_1 and f_2 have the right form.)

$$\dot{m}_{I,II,III} = \frac{Re_{I,II,III} \cdot \eta \cdot \delta \cdot F_{sc}}{D_{I,II,III}} \qquad (56)$$

(mass flow)

$$Pr = c_{He}\, \eta / \lambda \qquad (57)$$

(Prandl number)

$$Nu_{I,II,III} = \varphi_1 \cdot Re_{I,II,III}^{\varphi_2} \cdot Pr^{\varphi_3} \cdot (T_s / T_{He,i})^{\varphi_4} \,. \qquad (58)$$

Nu is the Nusselt number; C_1, C_2, C_3 and C_4 are constants taken from the literature; in general, they are different between conductor configurations I and II, III. In eq. (58) the expression in parenthesis, T_w/T_b (T_w is the wall temperature and T_b the temperature of the bulk cooling medium) has been replaced by T_s and $T_{He,i}$.
If C_1, C_2, C_3 and C_4 have the values 0.0256, 0.8, 0.4 and 0, the Dittus-Boelter correlation follows from eq. (58) and if the corresponding values are 0.0256, 0.8, 0.4 and 0.716 the empirical formula of Giarratano /17, 28/ is given.

The heat transfer coefficient follows from eq. (58):

$$h = Nu \cdot \lambda / D \qquad (59)$$

(the indices I, II and III are omitted).

$$Q_{BL} = \frac{c_{He}\, \gamma_{He}\, \lambda\, U\, \Delta x\, (T_s - T_{He,i})}{2\, h} \,, \qquad (60)$$

$$Q_s = \frac{T_s - T_{He,i}}{1/(h\,U\,\Delta x) + 1/(\dot{m}\,c_{He})} \cdot \Delta t \,, \tag{61}$$

$$Q_L = \frac{\Delta x}{2}\left[c_{He}\cdot\gamma_{He}\cdot\delta\cdot F_{sc} - C_{BL}\right]\frac{h\,U\,\Delta x\,(T_s - T_{He,i})}{\dot{m}\,c_{He} + h\,U\,\Delta x}\left[1-\exp\left(\frac{-h\,U\,\Delta t}{C_{He}}\right)\right], \tag{62}$$

$$Q_K = \left[C_{He}(1-\alpha_s)^2(T_c - T_{He,i}) - I^2\varrho_{ST}\,\Delta t/(\alpha F_{sc})\right]\Delta x \,, \tag{63}$$

$$\alpha_s = I^2\varrho_{ST}\frac{1}{\alpha F_{sc}\,U\,h\,(T_c - T_{He,i})} \,, \tag{64}$$

$$Q_{CO} = \Delta x\, F_{sc}\int_{T_{He,i}}^{\bar{T}_s}\left[C_{sc} + \alpha C_{ST} + \gamma C_{SO}\right]dT \,. \tag{43}$$

Q_i are the components of the critical energy (see Sec. 1) and α_s is the Stekly parameter. In eqs. (60-64) the indices I, II and III, for U, h, $\dot{m}$, and Q_i are omitted.

$$Q_\Omega = \varrho_{ST}\cdot j_c\cdot IK\cdot I\,\Delta x\,\Delta t/\alpha \tag{65}$$

(ohmic heat),

$$\xi = 4\cdot 10^{-7}\,\pi\,\eta_2\,R_1\,\Delta\,j_c\,IK/\left[B_m(R_1 + \Delta/2)\right] \,. \tag{66}$$

η_2 is the filling factor including the coil casing thickness, R_1 is the minimum distance of the TF coil centre line from the main torus axis, B_m is the maximum magnetic induction value at the inner TF coil edge and Δ is the radial thickness of the coil winding (see Fig. 4).

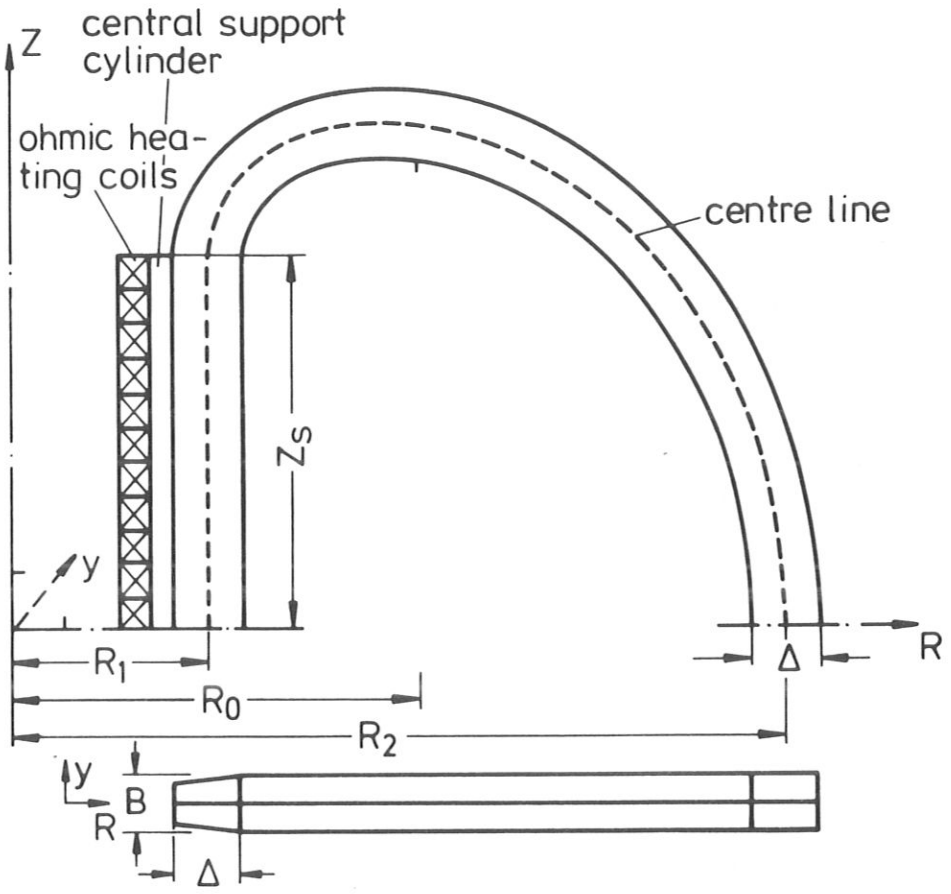

Fig. 4: Schematic view of a TF coil

$$\beta = [(1+\alpha)(\xi - 1 - \alpha - \gamma - \delta) + 0.25(2 + 2\alpha + \gamma + \delta - \xi)^2]^{1/2} - 0.5(2\alpha + 2 + \gamma + \delta - \xi) \quad (67)$$

ß is the average ratio of the cross-sectional area between the reinforcing material and superconductor.

$$Q_{ext} = P_{ext} F_{sc} (1 + \alpha + \beta + \gamma) \Delta x \Delta t \quad (68)$$

Q_{ext} is the heat deposited in the conductor from "external" sources such as a.c. fields or nuclear radiation; P is the power density.

The flow losses are calculated according to

$$P_{fl} = \dot{m} \Delta P \, 10^5 / \gamma_{He} \quad (69)$$

(ΔP in bar).

3. Structure of the FORCED program and the coupling to SUPERCOIL

FORCED will be used as a subprogram of the SUPERCOIL layout program /18/; it should be an alternative to the bath-cooling concept. In principle, the formulae described in the preceding section replace the relations (44), (51) and (52) from Ref. /18/. Relation (44) describes the "stability parameter" for a bath-cooled conductor which is optimized with respect to the bath-cooling stability criterion and safety discharge criterion. Relations (51) and (52) define α and β. In the FORCED program the α is calculated by the safety discharge criterion /2/; the stability and discharge criteria are "decoupled" (as a consequence both the conductor current and the current density can be used as independent parameters).

To calculate α and β some values have to be taken over from other parts of SUPERCOIL; these are: V_m, $E_{,m}$, η_2, Δ, $B = B_m$, R_1. (In Tables 5 and 6 the complete lists of the input and output data of FORCED are given.) The filling factor η_1, which takes into account the loss of winding area due to cooling, solder etc. is replaced in the β calculation (eq. 67) by

$$\eta_1 = 1 - \frac{\gamma + \delta}{1 + \alpha + \beta + \gamma + \delta} \,. \tag{70}$$

The critical energy depends on Δt, Δx and B; as far as B is concerned, difficulties are encountered in applying the force-cooling concept to TF coils because B strongly varies within the winding. There is an 1/R variation along the conductor and a nearly linear decrease of B across the radial thickness from the inner winding edge to the outer winding edge. As will be shown in the next section, Q_c decreases with increasing B. Thus for the layout calculation we take for B the maximum toroidal field value B_{max}, which is located at the inner coil edge $R = R_1 + \Delta/2$ (see Fig. 4).

As disturbance length Δx we choose the straight part of a D-coil, $\Delta x = 2L_S$, where L_S is taken from the part of SUPERCOIL which defines the geometry of the tokamak. There is another argument (besides the argument stemming from the influence of B on Q_c) for choosing the innermost conductor with length $2L_s$ for the layout calculation: The nuclear heat deposited in the conductor is largest at the inner coil edge.

Because the heat input is stationary (with respect to the transient cooling effects) and under stationary conditions the largest contribution to Q_c comes from Q_s (heat transferred away by the turbulent helium), Δt is a critical parameter. We choose for Δt (the duration time of the disturbance) the time which a helium fluid element needs to cover a distance $2L_S$:

$$\Delta t = 2L_s / v_{He} \quad (71)$$

where v_{He} is related to $\dot{m}$ in (eq. 56) by

$$v_{He} = \dot{m} / (\delta \cdot F_{sc} \cdot \gamma_{He}) \quad . \quad (72)$$

The helium mass follow depends on the total conductor length L. In our model L is the length of an unrolled pancake.

For the bundle conductor L is calculated from

$$L_I = 0.5\, L_o \Delta / [\beta F_{sc} / \pi + F_{sc}(1+\alpha+\gamma+\delta)/\pi]^{1/2} , \quad (73)$$

and for the hollow conductors

$$L_{II,III} = \frac{\Delta L_o}{F_{sc}^{1/2}\left\{\left[(1+\alpha+\gamma+\delta)/A\right]^{1/2} + \beta\left[(1+\alpha+\gamma+\delta)A\right]^{-1/2}\right\}} \quad , \quad (74)$$

A is the conductor aspect ratio A = a/b (see Fig. 12) and L_o is the circumference of the D-shaped centre line (see Fig. 4). L_o is calculated by the MAGNET subprogram of SUPERCOIL (eq. (72) in /18/).

As far as the input parameters are concerned (Table 5), it should be mentioned that there are three different groups. The first consists of parameters which define the structure of the conductor; these parameters are ICONC, ISPC and IST. ICONC defines the conductor concept; ICONC=1 denotes that the cable-in-conduit conductor (I) is taken into account, and ICONC=2 or 3 that hollow conductors with circular (II) or square (III) cooling channels are considered (see Fig. 3). ISPC defines the superconductor; ISPC=1 denotes that NbTi coils are simulated and ISPC=2 means that Nb_3Sn is used as superconductor. The parameter IST defines the stabilizer; IST=1 denotes that copper and IST=2 that aluminium is used as stabilizer.

The second group consists of input parameters marked with *. These are parameters which are taken from other subprograms of SUPERCOIL (such as E_m, V_m,...) or are input parameters (given in "by hand") for test runs (DX, THEAT, PHIT, BM).

The third group (without *) are input parameters for FORCED in the general sense.

The requirement for stable operation is that the critical energy be larger than the energy of the disturbance; this requirement is formulated by the heat balance equation (24).

The critical energy Q_c, if $\alpha_s > 1$, is calculated by summing up Q_{CO}, Q_{BL}, Q_L, and Q_S; if $\alpha_s \leq 1$ and the duration time Δt of the disturbance is small enough to yield $Q_K > 0$, Q_C is given by the sum of Q_{CO}, Q_{BL}, Q_L, Q_S and Q_K.

The critical energy Q_C is than compared with Q_{ext}; if Q_c is smaller than Q_{ext}, the critical energy Q_c has to be increased (or Q_{ext} decreased) until equality is obtained. There are several parameters influencing Q_c; for example, α , I, ΔP (and therefore $\dot{m}$, h) δ , B, Δx, Δt.

As variable parameters we use the conductor current I and ΔP; both have lower and upper bounds. Variations of ΔP produce variations in the helium mass flux $\dot{m}$ which has a strong influence on the critical energy /7, 23/. The requirement $Q_c \geq Q_{ext}$ for an optimized conductor is obtained by the following procedure. In order to determine whether stable operation can be achieved, the maximum attainable Q_c value is calculated by varying I between the upper limit $I = I_c = I_{max}$ (input parameter) and the lower limit $I = 0$. $Q_{c\ max}$ is given for $I = 0$ (see argumentation for the description of the results shown in Fig. 10). If Q_{ext} is greater than $Q_{c\ max}$, stable conductor operation cannot be achieved with the input parameters; one possibility of increasing $Q_{c\ max}$ is to increase ΔP (thus increasing $\dot{m}$). If $Q_{c\ max}$ is greater than Q_{ext}, I is increased until equality of Q_c and Q_{ext} is attained.

4. Some illustrative examples

To compare the experimental and theoretical results as a means of obtaining an insight into the variation of Q_c and Q_{ext} with the conductor parameters, the FORCED program is applied to a bundle (cable-in-conduit) conductor which was studied extensively by Junghans /7, 9, 10, 27/. First the influence of α is considered. For bath-cooled conductors, stability increases with increasing α (stability and discharge criteria for bath-cooled conductors with an additional "external" disturbance are derived in the Appendix I).

As an external disturbance, a heat source is assumed which heats up the conductor (superconductor, stabilizer, solder) and reinforcing material homogeneously like a nuclear heat source. The heating power is assumed to be 5×10^5 W/m³ (a factor of about 100 too large compared with a shielded superconducting magnet).

The following parameters are kept constant: I = 2520 A, $T_{He,i}$ = 4.92 K, B = 6 T, Δx = 0.5 m, Δt = 0.1 s, I_c = 4649 A, δ = 10.56, P = 9.35 bar, ΔP = 2.5×10^{-3} bar, L = 1.5 m, φ = 0, γ = 3.0, f_1 = 0.335, f_2 = 0.1, C_1 = 7.3×10^{-3}; C_2 = 1; C_3 = C_4=0, superconductor NbTi, stabilizer Cu, β = 0.0, P_{ext} = 5×10^5 W/m³ (parameter set used for Fig.5).

A friction factor f and a Nusselt number Nu are used according to the experimental results /27/ in the forms

$$f = 0.335 \; Re^{-0.1} \quad , \quad Nu = 0.0073 \; Re \tag{75}$$

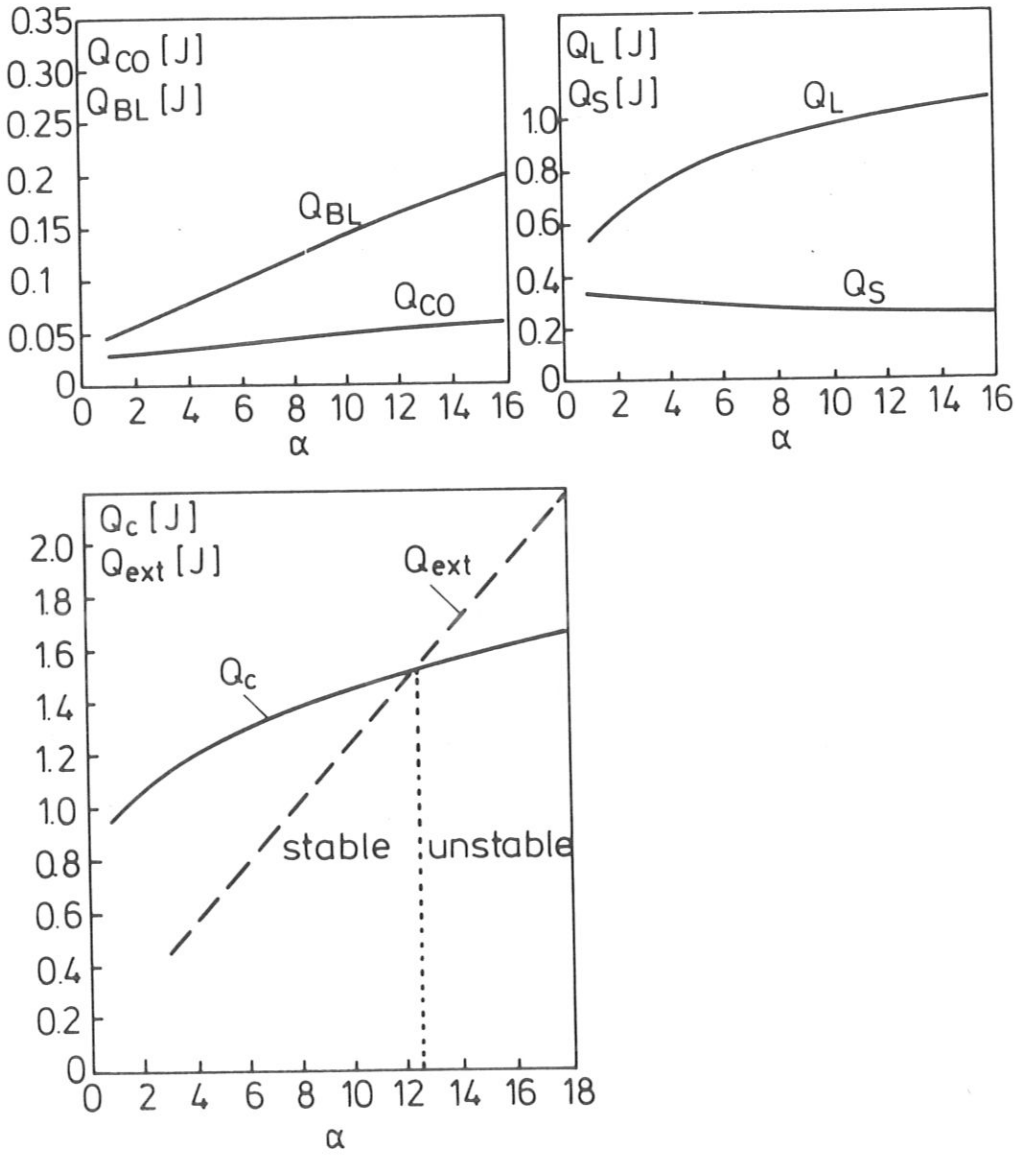

Fig. 5: Variation of the components Q_c, Q_s and Q_{ext} with α .

The variation of the critical energy $Q_c = Q_4 = \sum_4 Q_i$ of the components Q_i and of Q_{ext} is shown in Fig. 5. For a moment (when bath cooling is compared) the result is surprising; the stability increases with decreasing α ; which means that because F_{SC} is kept constant (I = const), the stability increases with decreasing amount of stabilizer (copper). The

reason for this behaviour is due to Q_{ext} decreasing with decreasing α more strongly than Q_c, which is dominated by the helium flow and not by the amount of material. (In this example no ohmic losses are taken into account.) In Fig. 6, the dependence of the critical energy on the magnetic field B is shown. This figure clearly demonstrates the problem when the force-cooling method is applied to superconducting TF coils, where B strongly varies within the coil winding. The variation of Q_c with B is mainly due to the influence of the magnetic induction B on T_s (see eqs. 26, 29). As B increases, T_s decreases (because T_c decreases) and also the difference $T_s - T_{He,i}$, which appears in the Q_i formula.

From the dependence of Q_c on B it follows that the most critical position in TF coils is the inner winding edge at $R = R_1 + \Delta/2$ (see Fig. 4). At this position, not only is the critical energy smaller but also the heat influx

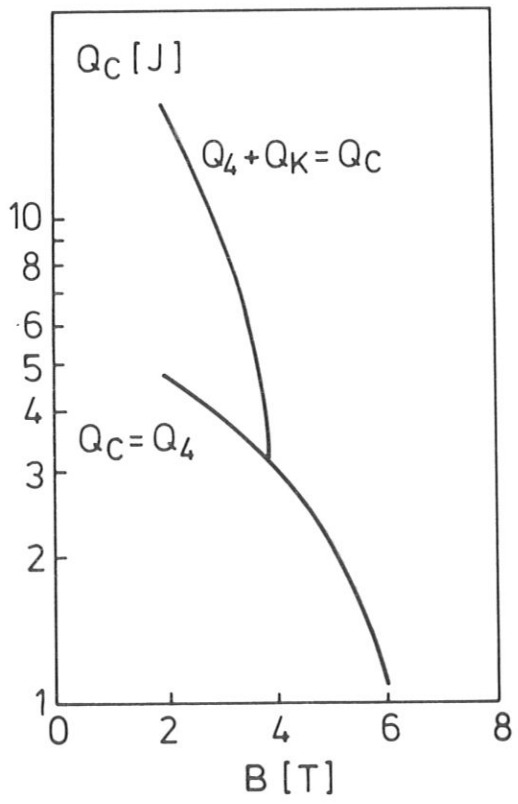

Fig. 6: Variation of the critical energy Q_c with the magnetic induction B. The parameters are the same as in Fig. 5 with the exception that α is kept constant at $\alpha = 3.96$.

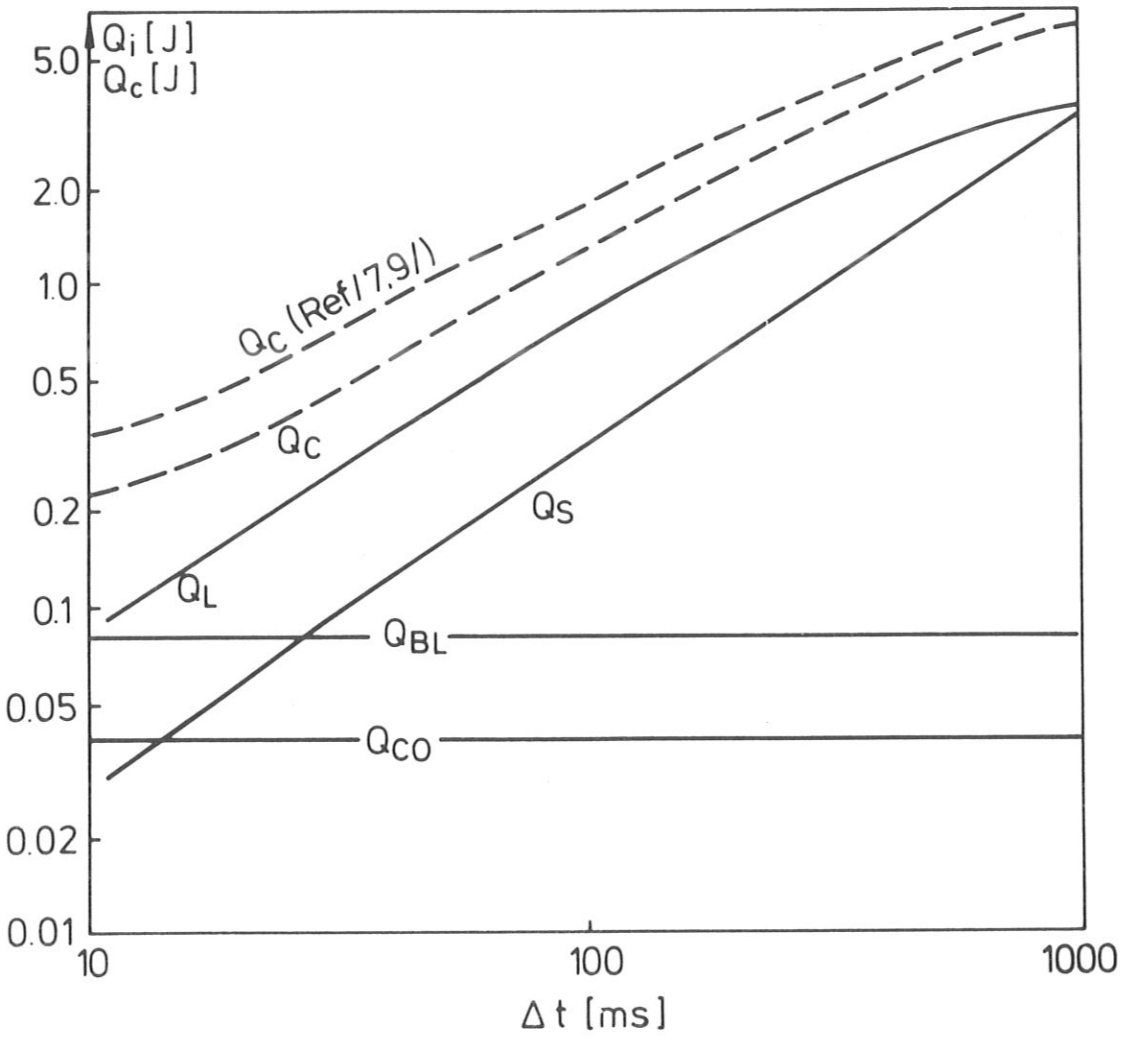

Fig. 7: Variation of Q_i and Q versus Δt. The Q_c-curve is compared with the corresponding curve from the literature /9/. The parameters are the same as in Fig. 5 with the exceptions α = 3.96 and B = 5 T.

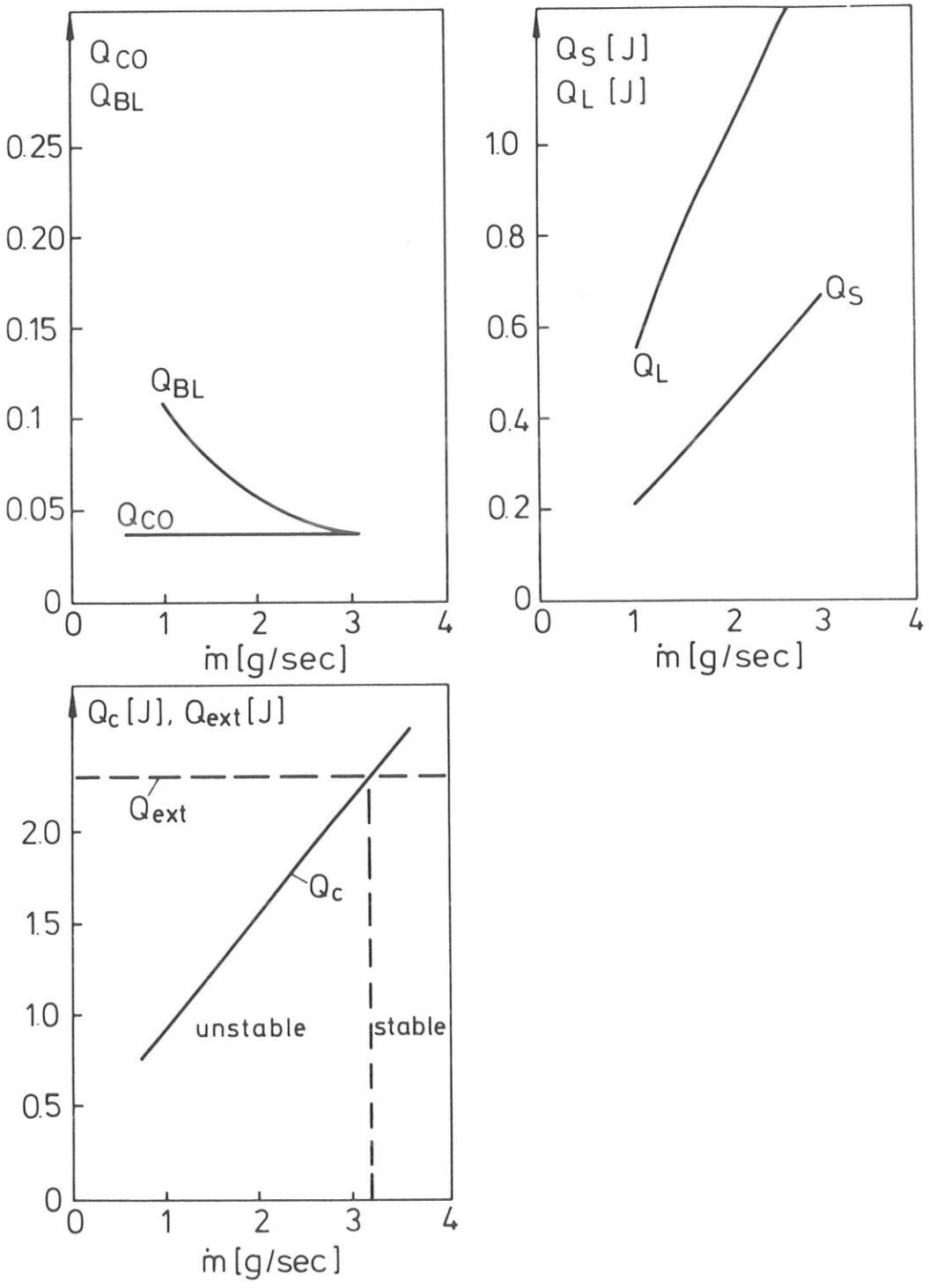

Fig. 8: Variation of the Q_i components ($1 \leq i \leq 4$) and the critical energy $Q_c = Q_4 = \sum_4 Q_i$ versus $\dot{m}$.

Data: see Fig. 5; changes: $\alpha = 3.96$; $\beta = 12.34$.

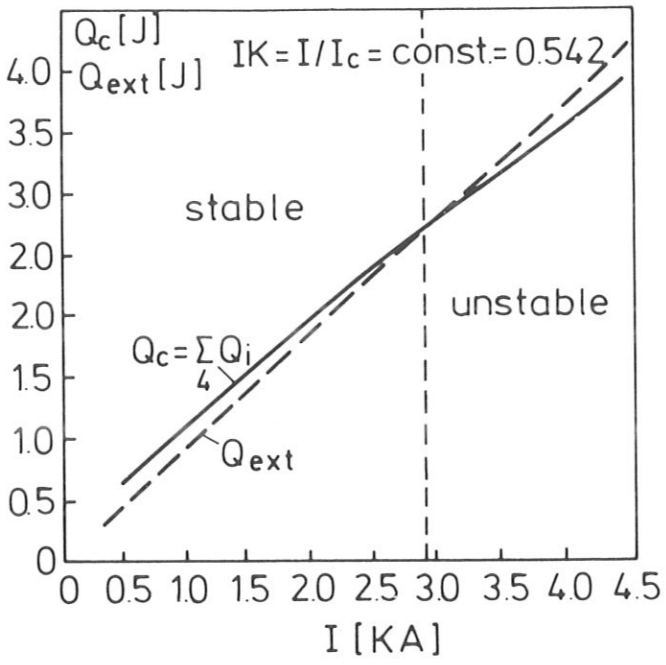

Fig. 9: Variation of the critical energy Q_c and the external energy Q_{ext} with conductor current. The ratio I/I_c is kept const = 0.542

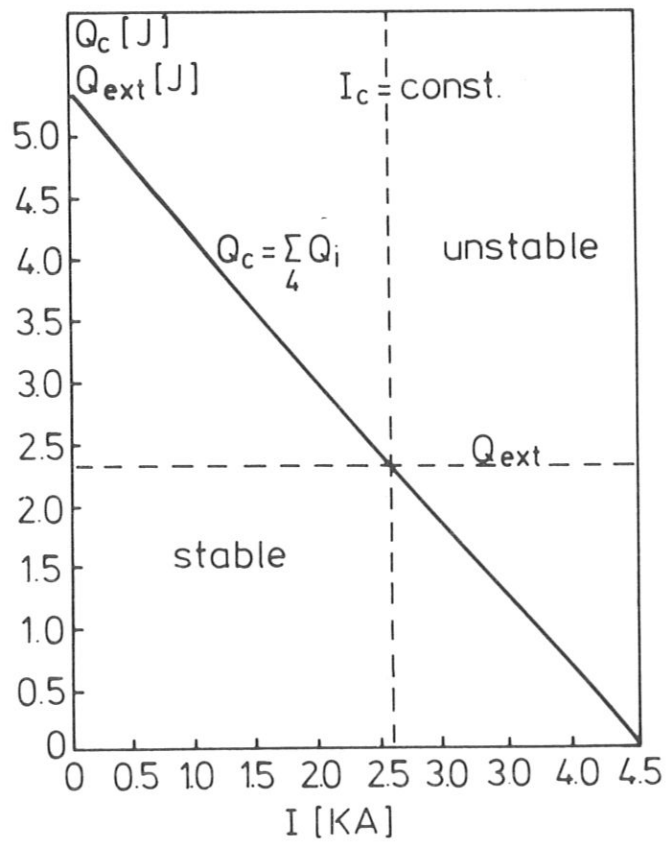

Fig. 10: Variation of Q_c and Q_{ext} with I for I_c = const = 4629 A.

produced by nuclear radiation is strongest. For these reasons we use for the layout calculations in SUPERCOIL the parameters at the inner coil edge ($B = B_{max}$, $\Delta x = 2L_S$, $\Delta t = 2L_S / v_{He}$, $\varphi = \varphi_n$). (Note that the force-cooling concept - in contrast to the bath-cooling concept - is not a local concept; Δx and Δt enter.)

The dependences of Q_c and Q_i on Δt are shown in Fig. 7; a comparison with the results of Refs. /7, 9/ is also made. The deviation of Junghans Q_c-curve from our curve depends on the material values, which are not described in Ref. /7, 9, 10/. If the strong influence of the superconducting properties (T_s, j_c) on Q_c is considerd the deviations are understandable.

As mentioned, the mass flow of the supercritical helium has a large influence on Q_c. By varying ΔP the $\dot{m}$ values can be changed; results are shown in Fig. 8.

In the following, the influence of the conductor current I on Q_c is discussed. The conductor current I (which is an input parameter) is varied from zero up to about 4600 A. The variation of I can be carried out in two ways, namely under the condition where I/I_c (I_c is the critical current) is kept constant (Fig. 9) and where I_c is constant (Fig. 10).

When I/I_c is kept constant and I varies, the critical current I_c also varies according to I/IK. The cross-sectional area of the superconductor F_{SC} depends on I_c as $F_{SC} = I_c / j_c(T,B)$, where j_c is the critical current densit of the superconductor. Changing I (IK = const) implies a change in F_{SC}; increasing I yields an increase in F_{SC}. The cross-sectional areas of

the stabilizer, cooling channels, etc. in our model are made proportional to F_{SC} ($\alpha, \beta, \gamma, \delta$ are the factors); increasing F_{SC} produces higher Q_c-values, as shown in Fig. 9. The disadvantage is that Q_{ext} also increases if "volume heat sources" are present, which is the case with nuclear heating. A procedure for finding an optimized conductor with $Q_c = Q_{ext}$ that is based on this procedure (I variable, I/I_c = const) is not suitable.

A better procedure is to change I but to keep I_c constant, which yields constant conductor dimensions and constant Q_{ext} values. This procedure better describes the actual operation of a superconducting coil. The conductor current I is changed within the natural limits ($0 \leq I \leq I_c$) until stable operation is attained ($Q_{ext} \leq Q_c$). As shown in Fig. 10, where the conductor current is varied between zero and I_c (I_c = 4629 A), the critical energy is zero for $I = I_c$ (because $T_s = T_c$) and has the maximum value at I = 0.

In Figs. 9 and 10, I was varied and IK or I_c was kept constant. Another optimization procedure can be defined if I is kept constant and IK is varied; the results are shown in Fig. 11. Q_c decreases with increasing IK. At IK = 1, the conductor current I is equal to I_c; there is no possibility of the conductor, including the helium, taking over heat ($T_s = T_{He}$), so that Q_c is zero. For IK smaller than 0.5 (see Fig. 11) the conductor is also stable when the temperature is larger than $T_s (Q_K > 0)$, and the total current I flows in the stabilizer.

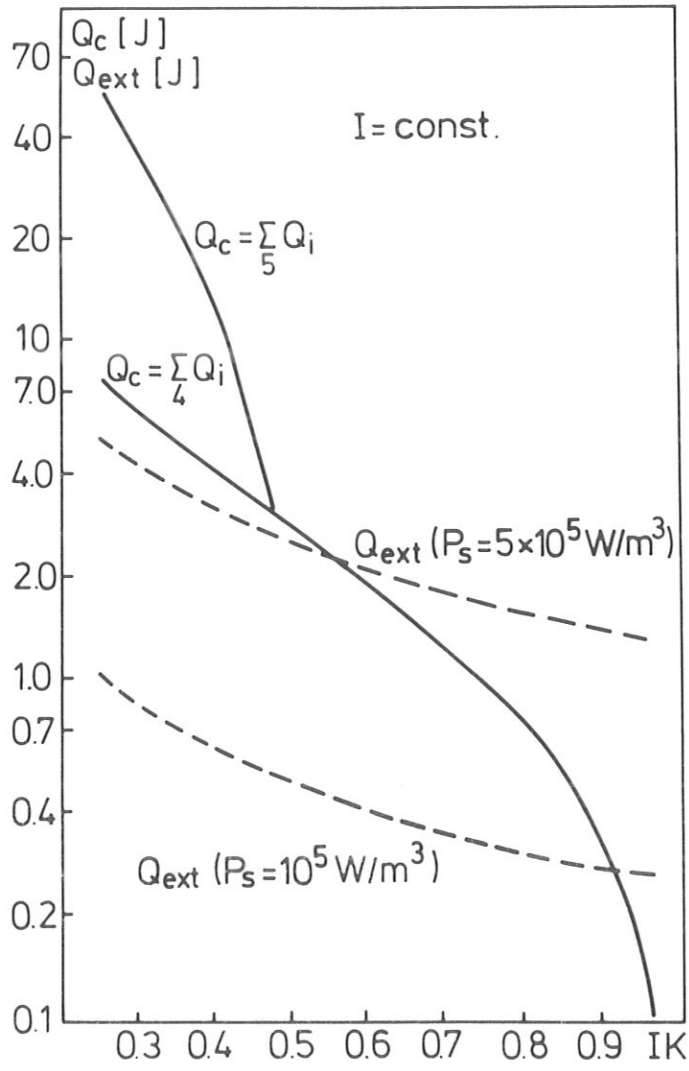

Fig. 11: Variation of Q_c and Q_{ext} with IK = I/I_c when I = const.

II. Model for a.c. loss calculations

Sections II and III describe the models for calculating the heat sources P which enter into the formula for Q_{ext}.

1. A.C. losses

The A.C. losses are composed of the hysteresis losses $P_{h\perp,\parallel}$, the eddy current losses $P_{e\perp,\parallel}$ in the stabilizer, and the coupling losses $P_{c\perp,\parallel}$. (The indices $\perp$ and $\parallel$ refer to the direction of the a.c. magnetic field with respect to the conductor direction; $\perp$ means, for instance, that the losses are produced by the magnetic field component $B_\perp$ perpendicular to the conductor direction).

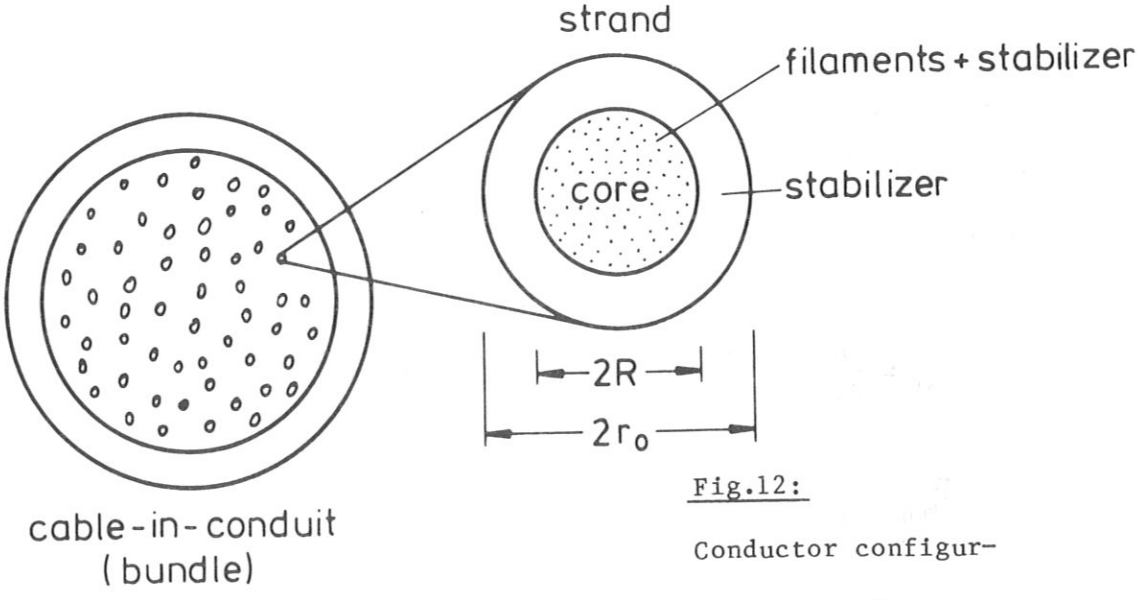

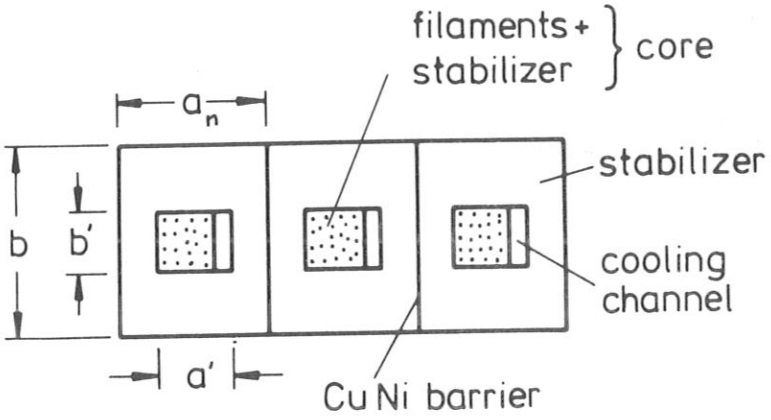

Fig.12: Conductor configurations for the a.c. calculation model. The hollow conductor consists of three (n = 3) subunits.

Figure 12 shows the conductor configurations for which the a.c. losses are calculated. The subdivision of the hollow conductor concept with n cooling ducts of circular or square cross-section (see Fig. 3) is simplified to one concept with one rectangular cross-sectional area. The formulae for the a.c. losses are based on the studies described in /5, 29/.

a) Bundle conductor

For the cable-in-conduit (bundle) conductor the following formulae are used:

$$r_o = \left[F_{sc} (1+\alpha) / \pi n \right]^{1/2} , \tag{76}$$

$$R = r_o \left[(1+\alpha_c) / (1+\alpha) \right]^{1/2} \tag{77}$$

(for r_o, R see Fig. 12; α_c is the ratio F_{ST}/F_{SC} in the strand core; α is the "global" ratio F_{ST}/F_{SC} calculated from the safety discharge criterion (41)).

$$P_{h\perp} = \frac{2}{3\pi} j_c \cdot d \cdot \dot{B}_\perp \cdot F_{sc} \qquad [W/m] , \tag{78}$$

$$P_{h\parallel} = \frac{1}{6} j_c \cdot d \cdot \dot{B}_\parallel \cdot F_{sc} \qquad [W/m]. \tag{79}$$

(hysteresis losses; d is the diameter of a superconducting filament; (term with $(I/I_c)^2$ is neglected; $(I/I_c)^2 \ll 1$).

$$P_{e\perp} = \frac{n\pi}{4\rho_{ST}} (r_o^4 - R^4) \dot{B}_\perp^2 \qquad [W/m] , \tag{80}$$

$$P_{e\parallel} = \frac{n\pi}{8\rho_{ST}} (r_o^4 - R^4) \dot{B}_\parallel^2 \qquad [W/m] \tag{81}$$

(eddy current losses produced in the stabilizer surrounding the strand core).

$$\rho_{eff} = \rho_{st} \cdot w/(w-d) \tag{82}$$

(effective specific resistance in the core; w = distance between the filaments; w/(w-d) is in the range of 2-5).

$$P_{c\perp} = n\pi R^2 (l_p/2\pi)^2 \left[\frac{1}{\rho_{eff}} + \frac{1}{\rho_{st}} \cdot \ln\left(\frac{r_0^2 - R^2}{R(R+r_0)}\right)\right] \dot{B}_\perp^2 \left[W/m\right] \tag{83}$$

$$P_{c\parallel} = \frac{n\pi^3}{6\rho_{st}} (l_a/l_p)^2 \dot{B}_{\parallel}^2 R^4 \quad \left[W/m\right] \tag{84}$$

(coupling losses; l_p is the twist length and l_a is the alternating twist length).

By calculating the a.c. losses of the total conductor with the formulae (78-84), the contributions from the single strands are added up. Within this model the mutual magnetic coupling of the strands has been neglected; the strands are also galvanically separated from each other.

b) Hollow conductor

The hysteresis losses are calculated with formulae (78, 79). The conductor geometry is defined by the aspect ratio A = a/b = a'/b' and a_n = a/n(see Fig. 12). The core with the superconducting filaments and a small amount of stabilizer (described in the model by α_c) is also rectangular in shape and has the aspect ratio A. The sides a', b' and a, b are given by

$$a' = [(1+\alpha_c+\delta) F_{sc} A/n]^{1/2}, \tag{85}$$

$$b' = [(1+\alpha_c+\delta) F_{sc}/(A\cdot n)]^{1/2}, \tag{86}$$

$$a_n = [(1+\alpha+\gamma+\delta) F_{sc} A/n^2]^{1/2}, \tag{87}$$

$$b = [(1+\alpha+\gamma+\delta) F_{sc}/A]^{1/2}. \tag{88}$$

The eddy current and coupling losses are

$$P_{e\perp} = \frac{n}{12\rho_{sT}} a_n^3 (b-b') \dot{B}_\perp^2 \qquad [W/m], \tag{89}$$

$$P_{e\parallel} = \frac{n}{16\rho_{sT}} \frac{(a_n+a')^2 (b+b')^2}{(a_n+b+a'+b')^2} (a_n b - b'a') \dot{B}_\parallel^2 \quad [W/m] \tag{90}$$

(eddy current losses). In deriving eq. (90) it is assumed that the induced electric field is constant in the region where only the stabilizer is present and the value is given by the contour integral over the average length s = a+b+a'+b'.

$$P_{c\perp} = (\alpha_c+1) F_{sc} (\ell_p/2\pi)^2 \left[\frac{1}{\rho_{eff}} + \frac{1}{\rho_{sT}} \ln\left[0.5 \frac{a_n b - a'b'}{a'b'}\right]\right] \dot{B}_\perp^2 \quad [W/m] \tag{91}$$

$$P_{c\parallel} = \frac{\pi}{6n} [F_{sc}(\alpha_c+1)]^2 \frac{1}{\rho_{sT}} (\ell_a/\ell_p)^2 \dot{B}_\parallel^2 \quad [W/m]. \tag{92}$$

If one applies a.c. loss formulae to conductors for large TF or PF magnet systems, one has to keep in mind the complexity of such condutors. The differences between measured and calculated ones can be rather high. Factors of 6-10 are found /33/ for the LCT conductor, where the a.c. losses

are calculated with theories based on an approach other than that used in this report. The underlying principle of the formulae used in this report is a "heterogeneous" structure consisting of a finite number of superconducting filaments (see Refs. 5, 29, 34). The other approach is based on the model that the twisted superconducting composite is a continuum with anisotropic properties /35, 36/. Improvements need advanced theories which are more adapted to the special conductor being used.

c) Stability criterion

The critical energy Q_c is calculated by formulae of the form $q_c \cdot \Delta x$, where q_c is the critical energy per unit length. The same structure is given for the a.c. losses. Q_{ext} follows from the a.c. losses as

$$Q_{ext} = (P_{h\perp} + P_{h\parallel} + P_{e\perp} + P_{e\parallel} + P_{c\perp} + P_{c\parallel}) \Delta x \cdot \Delta t \quad . \tag{93}$$

III. Model for nuclear heating

The nuclear heating power can be approximated within the TF coil region as

$$P = P_{max} \cdot exp(-x/\lambda), \tag{94}$$

where P_{max} is the peak value at the inside boundary ($R = R_1 + \Delta/2$) of the TF coil (see Fig. 4). Numerically absolute peak values P_{max} of about 3×10^2 W/m³ /30/ were found, where the shield thickness was 0.65 m; for λ a value of 0.0903 m was estimated /31/ by using the results of /30/.

An analytical formula for P_{max} can be deduced by using the formulae (24) and (27) for N_n (mean neutron wall load) and ϕ_n (neutron flux behind the shielding) in SUPERCOIL /18/:

$$P_{max} = 7.844 \cdot 10^5 \, N_n \cdot exp(-14.0 \, D) \tag{95}$$

(for D = 0.65 m, N_n = 1.3 MW/m² $\rightarrow$ P_{max} = 113 W/m³). In formula (95) only the fast neutrons (E > 0.1 MeV) are considered, whereas the numerical result include the total neutron flux, which is a factor of about 1.7 as high as the fast neutron flux, and the gamma flux. It thus seems to be a good approximation to multiply P_{max} from, for example, e.g. (95) by a factor of 2 or 3. As the example shows, the analytical p_{max} value then lies in the range of 226 - 339 W/m³ and fits the numerical result well.

As discussed in Sec. 3, the conductor placed at the inner coil boundary at $R = R_1 + \Delta/2$ is simulated for the stability calculation; P is therefore

replaced by P_{max}; within this model the distinction between the different absorption values of the conductor materials is not made; the P_{max} values are therefore average values.

The input data for the a.c. and nuclear heating calculation are collected in Table 7.

Appendix I

Bath-cooling with additional heat sources

The bath-cooling concept used up to now in SUPERCOIL is limited with respect to the heat sources; only the ohmic heat losses are considered. The stability criteria can be written in the form /1-5/

$$\varrho_{ST} \cdot j_{sT}^2 \cdot F_{ST} \leq \dot{q} \cdot \gamma_w \cdot U \,, \tag{96}$$

where U is the conductor perimeter and γ_w the wetting parameter. The value of γ_w is the fraction of the conductor being wetted. If the perimeter U is expressed as

$$U = k \left[F_{SC} + F_{ST} \right]^{1/2} \tag{97}$$

and F_{ST}/F_{SC} is set equal to α , the relation (92) can be written as

$$j_{sT} \leq \left[\frac{\alpha+1}{\alpha} \right]^{1/3} \left[\frac{\dot{q} \cdot \gamma_w \cdot k}{\varrho_{sT}} \right]^{2/3} I^{-1/3} \tag{98}$$

(I conductor current, $\dot{q}$ = heat flux).

If the approximation $F_{SC} << F_{ST}$ is used ($\alpha >> 1$)*, eq. (98) has the well-known form

---

* (For large cryogenically stabilized magnet systems the inequality $\alpha >> 1$ is always satisfied.)

$$j_{ST} \leq \left[\frac{\dot{q}\, \gamma_w\, k}{\rho_{sr}} \right]^{2/3} I^{-1/3} \quad . \tag{99}$$

The geometric factor k depends on the conductor shape. For a conductor with the aspect ratio A = a/b (see Fig. 12) k is

$$k = 2 \left(\sqrt{A} + 1/\sqrt{A} \right) , \tag{100}$$

and for a conductor with circular cross-section

$$k = 2\sqrt{\pi} \, . \tag{101}$$

With additional heat sources (volume sources) $P_2 \ldots P_n$ and on the assumption that $\alpha >> 1$, the current density j_{ST} in the stabilizer is related to the conductor current as

$$j_{sr}^2 = \left(\frac{\dot{q}\, \gamma_w\, k}{\rho_{ST}} \right) j_{sr}^{1/2} I^{-1/2} - \frac{P_1 + \ldots + P_n}{\rho_{sr}} \quad . \tag{102}$$

In general, the ohmic heating is much higher than other heating sources. An example: the ohmic heating of a cryogenically stabilized conductor (according to eq. (99)) with the data $\rho_{ST} = 4 \times 10^{-10}\ \Omega m$, $\gamma_w = 0.5$, $k = 4.24$ ($a = 2b$), $I = 10^4\ A/m^2$, $\dot{q} = 3 \times 10^3\ W/m^2$) is about $3 \times 10^5\ W/m^3$; the maximum heating due to nuclear radiation for a shielded (65 cm) TF coil system is in the range of $3 \times 10^2\ W/m^3$ /30/. In this case the reduction of j_{ST} due to nuclear heating is small.

The safety discharge criterion /3/ when only the ohmic losses are involved can be written as

$$j_{ST} \leq \left[f(T_m)\, V_m\, I / E_m \right]^{1/2}, \tag{103}$$

with

$$f(T_m) = \int_{T_{He}}^{T_m} C_{ST} / \varrho_{ST}\, dT, \tag{104}$$

where C_{ST} is the specific heat per volume, ϱ_{ST} the specific resistance, V_m the maximum discharge voltage and E_m the stored magnetic energy.

The current density j_{ST} which follows from the expression (98) or (99) decreases with increasing conductor current I as $I^{-1/3}$, whereas the current density which follows from the discharge criterion increases as $I^{1/2}$. There exists one j_{ST} which meets both criteria; for this situation an optimum current density j_{opt} and an optimum corresponding conductor current I_{opt} are defined:

$$j_{opt} = \left[f(T_m)\, V_m / E_m \right]^{1/5} \left[\dot{q}\, \gamma_w\, k / \varrho_{ST} \right]^{2/5}, \tag{105}$$

$$I_{opt} = \left[f(T_m)\, V_m / E_m \right]^{-3/5} \left[\dot{q}\, \gamma_w\, k / \varrho_{ST} \right]^{4/5}. \tag{106}$$

(Note: the bath-cooling concept used in SUPERCOIL is based on this optimization procedure; I cannot be an input parameter, it follows from the model calculations. The situation is different in FORCED. Here the α value follows from the discharge criterion (103) at a given conductor current I; then the current density is calculated.)

The formulae (103-106) are derived /3/ on the assumption that the current j_{ST} varies during the safety discharge as $j = j_o\, e^{-t/\tau}$, where $\tau = L/R$ is the time constant of the discharge, (R being the resistance of the external shunt and L the inductance of the coil system: $E_m = 1/2\ LI^2$).

If there are additional heat sources during the safety discharge, one can imagine that high a.c. losses occur because strong magnetic induction variations B are produced during the discharge, the initial equation for the discharge criterion is

$$\int_0^{\infty} \left(j_{sT}^2 + P_{ac}/\varrho_{sT} \right) dt = \int_{T_{He}}^{T_m} C_{sT}/\varrho_{sT}\, dT. \qquad (107)$$

The eddy current losses (and coupling losses (see Section II) increase with B^2, and B varies with $j \propto e^{-t/\tau}$. The time dependence of P_{ac} is given by

$$P_{ac} = K \exp(-2t/\tau), \qquad (109)$$

where K contains the parameter of the a.c. loss formulae and τ.

For internally cooled superconductors with a low amount of stabilizing material the superconductor and solder have also to be taken into account in the discharge condition. The heat balance equation is then given by

$$\frac{1}{F_{sc}} \int_0^{\infty} \varrho_{sT}\, I^2\, dt = \int_{T_{He}}^{T_m} \left[C_{sc} F_{sc} + C_{sT} F_{sT} + C_{so} F_{so} \right] dT. \qquad (110)$$

Using the quantities E_m, V_m and γ ($\gamma = F_{SO}/F_{SC}$) and introducing the abbreviations for the integrals as done for eqs. (39, 40), the eq. (110) can be written as

$$\alpha F_m^{sc} + \alpha^2 F_m^{sT} + \alpha \cdot \gamma \cdot F_m^{so} = \frac{j_c^2 \cdot I K^2}{V_m I}. \qquad (111)$$

Appendix II

Dependence of the Stekly parameter on the temperature in the current shearing regime

Between T_s and T_c the ohmic heating power increases linearlily with temperature; experimental and theoretical investigations confirm this

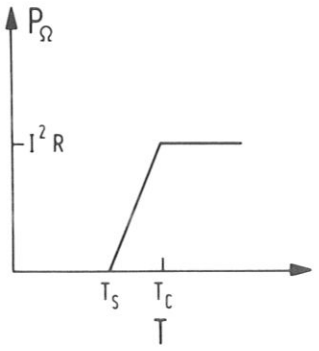

Fig. 12

Dependence of the ohmic heating power P on temperature.

dependence. At the critical temperature P is given by I^2R where I is the conductor current and R is the ohmic resistance (in x direction).

The Stekly parameter at $T = T_c$ is given by

$$(1 + \Delta d_S) = \frac{I^2R + P_1 + P_2}{h\, U\, (T_c - T_{He,i})} \qquad (22')$$

where P_1 and P_2 are "external heat sources".

Using the relation

$$P_\Omega = I^2R\ (T - T_S)/(T_c - T_S), \qquad (112)$$

$$I^2R = (1 + \Delta d_S)\, h\, U\, (T_c - T_{He,i}) - P_1 - P_2 \qquad (113)$$

$$P_1 + P_2 = h\, U\, (T_s - T_{He,i}) \tag{114}$$

the ratio $\Delta P_\Omega / \Delta P_c$ (where ΔP_Ω is the increase of the ohmic heating due to a temperature increase from T_s to $T_s + \Delta T$ and ΔP_c is the increase of the cooling by an increase of the heat transfer) is given by

$$\Delta P_\Omega / \Delta P_c = 1 + \Delta\alpha_s \frac{T_c - T_{He,i}}{T_c - T_s} \tag{115}$$

Equation (115) shows that for $\alpha_s = (1 + \Delta\alpha_s) > 1$ the increase of ΔP_Ω is larger than ΔP_c; the conductor is not stable if the temperature increases above the saturation temperature T_s. In calculating Rel. (115) it is assumed that at $T = T_s$ the external heat sources are compensated by the heat carried away by the helium (eq. 112) and h is independent of the temperature (see eqs. (58), (59)).

Acknowledgement

The author thanks K. Borraß for usefull discussions and suggestions and H. Gorenflo for the help in developing the computerprogram ZWANGSK.

Table 1: Density γ_{He} of supercritical helium [kg/m³K]

P[bar]→4 T[K]		6	8	10	12	16	20	30	40
4	141.0	145.9	149.8	153.1	156.1	161.1	165.4	174.0	181.0
5	124.2	132.9	138.9	143.6	147.6	153.9	159.0	169.0	
6	82.6	112.3	123.7	131.1	136.7	145.0	151.4	163.0	171.5
7	42.6	78.5	102.0	114.7	123.2	134.6	142.7	156.5	
8	31.4	54.1	76.6	94.5	106.8	122.5	132.8	149.3	160.2
10	22.1	35.1	49.0	62.4	74.7	95.5	110.4	133.3	147.3
12	17.4	27.0	36.9	46.9	56.5	74.0	89.1	116.1	133.4
14	14.5	22.2	30.0	37.9	45.7	60.5	73.8	100.1	119.6
16	12.5	18.9	25.4	32.0	38.5	51.1	62.9	87.9	107.2
20	9.8	14.7	19.7	24.6	29.5	44.3	48.4	77.7	87.3

Table 2: Specific heat of supercritical helium [J/kgK]

P[bar]→4 T[K]		6	8	10	12	16	20	30	40
4	3242	30005	2842	2718	2618	2459	2336	2112	1957
5	5528	4502	4038	3756	3559	3292	3111	2825	2649
6	16890	7072	5452	4763	4364	3900	3626	3239	3024
7	10050	11380	8045	6362	5523	4684	4250	3704	3425
8	7547	9181	9326	8114	6935	5611	4954	4191	3831
10	6252	6913	7419	7633	7668	7111	6330	5161	4612
12	5863	6226	6542	6757	6865	6893	6734	5913	5285
14	5674	5921	6145	6323	6446	6538	5610	6172	5716
16	5556	5739	5909	6056	6173	6310	6342	6186	5911
20	5419	5530	5636	5734	5822	5959	6044	6088	6003

Table 3: Thermal conductivity λ of supercritical helium [W/mK]

P[bar]→ T[K] ↓	4	6	8	10	12	16	20	30	40
4	0.0215	0.0223	0.0231	0.0237	0.0243	0.0254	0.0263	0.0284	0.0302
5	0.0222	0.0237	0.0249	0.0258	0.0267	0.0281	0.0294	0.0320	0.0342
6	0.0215	0.0235	0.0253	0.0268	0.0280	0.0300	0.0316	0.0348	0.0375
7	0.0174	0.0218	0.0246	0.0266	0.0283	0.0309	0.0329	0.0369	0.0400
8	0.0174	0.0201	0.0230	0.0256	0.0277	0.0309	0.0334	0.0381	0.0418
10	0.0190	0.0205	0.0222	0.0240	0.0259	0.0296	0.0328	0.0388	0.0433
12	0.0209	0.0219	0.0231	0.0244	0.0258	0.0287	0.0316	0.0381	0.0432
14	0.0227	0.0236	0.0246	0.0256	0.0267	0.0291	0.0315	0.0373	0.0426
16	0.0244	0.0252	0.0260	0.0269	0.0279	0.0294	0.0319	0.0371	0.0420
20	0.0276	0.0283	0.0290	0.0297	0.0304	0.0319	0.0335	0.0376	0.0417

Table 4: Viscosity η of supercritical helium [kg/ms] x 10^5

P[bar]→ T[K] ↓	4	6	8	10	12	16	20	30	40
4	40.0	43.7	47.1	50.4	53.6	59.8	66.1	82.0	99.1
5	33.6	37.6	41.0	44.0	46.9	52.3	57.5	70.3	83.4
6	25.5	32.1	36.0	39.1	41.8	46.8	51,4	62,3	73.0
7	22.2	27.2	31.8	35.3	38.1	42.9	47.1	56.7	65.9
8	22.8	25.8	29.1	32.4	35.2	39.9	44.0	52.8	61.0
10	25.1	27.0	28.9	30.8	32.7	36.6	40.1	49.9	54.7
12	27.6	29.0	30.5	31.9	33.3	36.1	38.8	47.8	51.3
14	30.1	31.3	32.4	33.6	34.8	37.1	39.3	45.3	49.7
16	32.5	33.5	34.5	35.5	36.5	38.5	40.4	44.6	49.4
20	37.0	37.8	38.6	39.4	40.2	41.8	43.3	47.0	50.5

Table 5: Complete list of input data (notation used in the FORCED computer program)

Program	Dim.	Description	Notation in this report
ALFA[+)]		ratio F_{ST}/F_{SC}	α
IC	(A)	conductor current	I
TH	(K)	helium temperature at inlet	$T_{He,i}$
BM[+)]	(T)	magnetic induction	B
DX[+)]	(m)	length of perturbation	Δx
ICRI	(A)	critical current	I_c
THEAT[+)]		duration of perturbation	Δt
CROSS		ratio $F_{cooling}/F_{SC}$	δ
CSOL		ratio F_{SO}/F_{SC}	γ
P	(bar)	pressure at inlet	P
DELP	(bar)	pressure drop	ΔP
LO	(m)	conductor length	L
PHIT[+)]	(m^{-2})	neutron flux	ρ
F1		) coefficients for the	f_1
F2		) friction factor	f_2
CNU1		)	C_1
CNU2		) coefficients for the	C_2
CNU3		) Nusselt number	C_3
CNU4		)	C_4
E[+)]	(J)	stored magnetic energy	E_m
VM[+)]	(V)	maximum discharge voltage	V_m
TM	(K)	maximum conductor temperature after a safety discharge	T_m
R1[+)]	(m)	minimum distance of the centre line for main torus axis	R_1
DEL[+)]	(m)	radial winding thickness of the TF coil	Δ
ETA2[+)]		filling factor	η_2
NN		number of strands for conductor I number of channels for conductor II, III	
ICONC = 1,2,3		conductor concept;	I,II,III
ISPC = 1,2		1 NbTi; 2 Nb_3Sn superconductor	
IST = 1,2		1 copper; 2 aluminium stabilizer	

+) The data are taken from SUPERCOIL or can be calculated internally like Δt

Table 6: Main output data

Program name	Dim.	Description	Notation in this report
TC	(K)	critical temperature	T_c
T_S	(K)	saturation temperature	T_s
JC	(A/m^2)	critical current density	j_c
REY		Reynolds number	Re
QCOEF	(W/m^2K)	heat transfer coefficient	h
QME	(J)	equ. 43	Q_{co}
QBL	(J)	equ. 60	Q_{BL}
QS	(J)	equ. 61	Q_s
QL	(J)	equ. 62	Q_L
ALFA		ratio F_{ST}/F_{SC}	α
BETA		ratio F_R/F_{ST}	ß
AS		Stekley parameter	α_s

Table 7: Additional input parameters for the a.c. and nuclear heat deposition calculations

Program name	Dim.	Description	Notation in this report
ALFAS		ratio F_{ST}/F_{SC} in the core	$_s$
A		conductor aspect ratio	A
TWL+)	(m)	twist length	l_p
D+)	(m)	shielding thickness	D
DF+)	(m)	filament diameter	d
NW+)	(MW/m^2)	wall loading	N_n
BPD+)	(T/s)	magnetic field variation with time perpendicular to the conductor	$\dot{B}_\perp$
BPS+)	(T/s)	magnetic field variation with time parallel to the conductor	$\dot{B}_\parallel$
NS		number of strands for conductor configuration I or subdivision number of the hollow conductor (NS = can be set equal to NN).	n

References

/1/ Z.J.J.Stekly, J.L.Zar: "Stable superconducting coils", IEEE Transaction on Nuclear Science NS 12/3 (1965) 367

/2/ B.J. Maddock, G.B. James: "Protection and stabilization of large superconducting coils", Proc. IEE 115 (1968) 543

/3/ B.J. Maddock, G.B. James, W.T. Norris: "Superconducting composites: heat transfer and steady state stabilization", Cryogenics 9 (1969) 261

/4/ M.N. Wilson, Y. Iwasa: "Stability of superconductors against localized disturbances of limited magnitude", Cryogenics 18 (1978) 17

/5/ H. Brechna: "Superconducting Magnet Systems", Springer Verlag Berlin 1973

/6/ M. Mopurgo: "Review of work done at CERN on superconducting coils cooled by a forced circulation of supercritical helium", Proc. 3rd Int. Conf. on Magnet Technology, Hamburg 1970, p. 908

/7/ D. Junghans: "Stabilität forciert gekühlter Supraleiter", SIN-Bericht TM-31-05, 1982

/8/ G. Pasztor, C. Schmidt: "Dynamic stress effects in technical superconductors and the 'training' problem of superconducting magnets", J.Appl.Phys. 49/2 (1978) 886

/9/ D. Junghans: "Stability of force-cooled superconductors. Part I: Theory", Cryogenics 23 (1983) 220

/10/ D. Junghans: "Stability of force-cooled superconductors. Part II: Experiment", Cryogenics 23 (1983) 227

/11/ A.Y. Lee: "Cryogenic recovery analysis of forced-flow supercritical-helium-cooled superconductors", Adv. Cryog. Eng. 23 (1978) 235

/12/ J.K. Hoffer: "The initiation and propagation of normal zones in a force-cooled tubular superconductor", IEEE Trans. on Mag. MAG-15 (1979) 331

/13/ C. Marinucci: "A numerical model for the analysis of stability and quench characteristics of forced-flow-cooled superconductors", Cryogenics 23 (1983) 579

/14/ J. Benkowitsch, G. Krafft: "Numerical analysis of heat-induced transients in forced flow helium cooling systems", Cryogenics 20 (1980) 209-215

/15/ G. Krafft, G. Ries: "Quench studies on the Euratom-LCT conductor", 8th Cryog. Eng. Conf. (1980), p. 330

/16/ G. Krafft, G. Zahn: "Experimental and theoretical investigations of heat-induced transients in forced-flow helium cooling systems", Proc. 8th Symp. on Eng. Probl. of Fus. Research, San Francisco 1979, p. 1724

/17/ VDI-Wärmeatlas, Berechnungsblätter für den Wärmeübergang, VDI-Verlag GmbH, Düsseldorf 1975

/18/ K. Borrass, M. Söll: "Supercoil, a Layout Model for Tokamaks with Superconducting TF Coils", Max-Planck-Institut für Plasmaphysik Garching, Report IPP 4/207, June 1982

/19/ J.W. Lue, J.R. Miller, L. Dresner: "Stability of cable-in-conduit conductors", J.Appl.Phys. 51/1 (1980) 772

/20/ L. Dresner: "Stability of cable-in-conduit, force-cooled conductors: Elementary Theory", Oak Ridge Nat. Lab., Report ORNL/TM-6657, 1979

/21/ M.S. Lubell: "Empirical scaling formulas for critical current and critical field for commercial NbTi", IEEE Tr. on Magnetics, MAG-19 (1983) p. 754

/22/ L.R. Turner, M.A. Abdou, "Computational model for superconducting toroidal-field magnets for a tokamak reactor", Proc. 7th Symp. on Eng. Probl. of Fus. Res., 1977, p. 762

/23/ W. Herz: "Results of the European LCT coil in the TOSKA facility" Proc. IEEE Tr. on Magnetics, MAG-21/2 (1985) 249

/24/ M. Söll: "Influence of radiation damage on the maximum attainable magnetic field for toroidal fusion magnet systems", J.Nucl.Mat. 72 (1978) 168

/25/ F.R. Fickett: "A review of resistive mechanisms in aluminium", Cryogenics 11 (1971) 349

/26/ R.D. McCarthy: "Thermophysical properties of helium-4 from 2 to 1500 K with pressures to 1000 atmospheres", National Bureau of Standards, Technical Note 631, 1972

/27/ D. Junghans: "Measurements of pressure drop, heat transfer coefficient and critical energy of a bundle conductor", IEEE Tr. on Magnetics, 17/5 (1981) 2209

/28/ F. Stelzer: "Wärmeübertragung und Strömung", Karl Thiemig AG, München (1971).

/29/ C-H. Dustmann et al.: "Supraleitungstechnologie für Fusionsmagnete", Gesellschaft für Kernforschung M.B.H Karlsruhe, Report KFK 2359 (1976)

/30/ W. Dänner: "Neutronics results for superconducting coils", The NET Team Garching, Report NET/IN/84-067 (1984)

/31/ R. Flükiger et al.: "An A15 superconductor design and its implications for the NET-II TF coils". Kernforschungszentrum Karlsruhe, Report EUR FU XII/361-85/3 (1985

/32/ J. Raeder et al.: "Kontrollierte Kernfusion", Teubner Studienbücher, Stuttgart 1981, 223-243

/33/ C. Schmidt: "Critical current, stability and a.c.-loss measurement on the EURATOM LCT conductor, IEEE Tr. on Magnetics, Vol. Mag.-19/3 (1983) 707

/34/ G.H. Morgan: "Theoretical behaviour of twisted multicore superconducting wire in a time-varying uniform magnetic field", J.Appl. Phys. 41 (1970) 3673

/35/ W.J. Carr: "a.c. loss in a twisted filamentary superconducting wire", J.Appl.Phys. 45 (1974) 929

/36/ V.B. Zenkevitch, A.S. Romaniuk: "Losses in multifilamentary superconductors at low levels of excitations", IEEE Tr. on Magnetics, MAG 13/1 (1977) 567